Combined tectonic-sediment supply-driven cycles in a Lower Carboniferous deep-marine foreland basin, Moravice Formation, Czech Republic

ARTICLE *in* INTERNATIONAL JOURNAL OF EARTH SCIENCES · MARCH 2004

Impact Factor: 2.09 · DOI: 10.1007/s00531-004-0388-5

Ondrej Bábek
Palacký University of Olomouc

Radek Mikuláš
Academy of Sciences of the Czech Republic

Tomáš Lehotský
Palacký University of Olomouc

Int J Earth Sci (Geol Rundsch) (2004) 93:241–261
DOI 10.1007/s00531-004-0388-5

ORIGINAL PAPER

Ondřej Bábek · Radek Mikuláš · Jan Zapletal · Tomáš Lehotský

Combined tectonic-sediment supply-driven cycles in a Lower Carboniferous deep-marine foreland basin, Moravice Formation, Czech Republic

Received: 28 June 2002 / Accepted: 14 December 2003 / Published online: 18 March 2004

Abstract The Lower Carboniferous Moravian–Silesian Culm Basin (MSCB) represents the easternmost part of the Rhenohercynian system of collision-related, deep-water foreland basins (Culm facies). The Upper Viséan Moravice Formation (MF) of the MSCB shows a distinct cyclic stratigraphic arrangement. Two major asymmetric megacycles bounded by basal sequence boundary, each about 500 to 900 m thick, have been revealed. The megacycles start with 50- to 250-m-thick, basal segments of erosive channels: overbank successions and slope apron deposits interpreted as lowstand turbidite systems. Up-section they pass into hundred metre-thick, fine-grained, low-efficiency turbidite systems. Palaeocurrent data show two prominent directions, basin axis-parallel, SSW–NNE directions, which are abundant in the whole MF, and basin axis-perpendicular to oblique, W–E to NW–SE directions, which tend to be confined to the basal parts of the megacycles or channel-lobe transition systems in their upper parts. Based on the facies characteristics, palaeocurrent data, sandstone composition data and trace-fossil distribution data, we suggest a combined tectonics–sediment supply-driven model for the MF basin fill. Periods of increased tectonic activity resulted in slope oversteepening probably combined with increased rate of lateral W–E sediment supply into the basin, producing the basal sequence boundary and the subsequent lowstand turbidite systems. During subsequent periods of tectonic quiescence, the system was filled mainly from a distant southern point source, producing the thick, low efficiency turbidite systems. Consistently with the previous models, our own sediment composition data indicate a progressively increasing sediment input from high-grade metamorphic and magmatic sources up-section, most probably related to an uplift in the source area and progressive unroofing of its structurally deeper crustal parts. The first occurrence of the Cruziana–Nereites ichnofacies in sand-rich turbidite systems in the youngest parts of the MF (Goβel to Goβspi Zone), supported by rapidly increasing quartz concentrations in sandstones, is thought to indicate a transition from generally underfilled to generally overfilled phase in evolution of the MSCB basin. This transition may be linked to the onset of Upper Viséan phase of northward basin-fill progradation assumed by previous authors.

Keywords Facies analysis · Foreland basin · Rhenohercynian Zone · Sediment provenance · Trace fossils

O. Bábek (✉) · J. Zapletal · T. Lehotský
Dept. of Geology, Palacký University,
tř. Svobody 2s6, 77146 Olomouc, Czech Republic
e-mail: babek@prfnw.upol.cz

R. Mikuláš
Geological Institute of Czech Academy of Sciences,
Rozvojová 135, 16500 Praha 6, Czech Republic

Introduction

Lower Carboniferous peripheral foreland basins filled with deep-water siliciclastics (Culm facies) are well documented from outcrop and subsurface of the Rhenohercynian Zone of Western and Central Europe (Franke and Engel 1988; Hartley and Warr 1990; Burne 1995; Ricken et al. 2000; Hartley and Otava 2001; Fig. 1). The basins evolved in response to the closure of the Rhenohercynian (Lizard–Giessen–Harz) ocean and subsequent continental collision spanning from the Frasnian to Westphalian interval (Franke 1995). In the Moravo–Silesian region at the eastern margin of the Bohemian Massif, the Culm facies are preserved in two major basins: the Drahany Basin and the Nízký Jeseník Basin (Fig. 2), which represent the easternmost parts of the Rhenohercynian Zone (Dvořák and Paproth 1969; Franke 1995). The two basins were filled with up to 12-km-thick successions of deep marine siliciclastics and they were most probably connected as suggested by their similar palaeocurrent and clastic provenance patterns (Kumpera and Martinec 1995; Hartley and Otava 2001).

The Drahany Basin located southward represents a more proximal part of the originally united basin fill (the

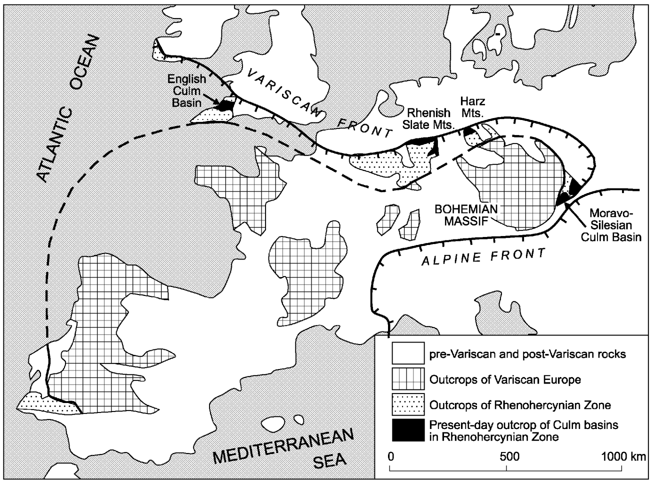

Fig. 1 Outcrops of Variscan flysch (Culm) basins in the Rhenohercynian Zone of Europe

Moravo-Silesian Culm basin, MSCB), whereas the Nízký Jeseník Basin located northward represents its distal part. Kumpera and Martinec (1995) interpreted the filling of the MSCB as a multiphase geotectonic event, which they subdivided into an initial, remnant basin phase (Lower to Middle Viséan) and a subsequent peripheral foreland basin phase (Upper Viséan to lowermost Namurian). During the foreland basin phase of the MSCB, the deep-water siliciclastics were deposited in a elongate submarine fan, fed from a point source located in the southern part of the Drahany Basin, whose stratigraphic architecture was controlled mainly by sediment supply (Kumpera and Martinec 1995; Hartley and Otava 2001). This interpretation is based mainly on the proximal-to-distal grain-size relationship, palaeocurrent data indicating northward sediment dispersal from the Drahany to the Nízký Jeseník Basin and similar detrital heavy mineral spectra in sandstones from both basins (Hartley and Otava 2001).

However, the presumably outer-fan fine-grained successions comprising the Upper Viséan Moravice Formation (MF) of the Nízký Jeseník Basin contain local accumulations of relatively thick, coarse-grained conglomerate bodies and infrequent, but important W–E to NW–SE, basin axis-perpendicular palaeocurrent directions. Supported with rather high variability in conglomerate clast composition (Zapletal 1986) and variability in ichnofacies characteristics (Zapletal and Pek 1999) these facts seem to be in contradiction with the published, simple fan model of the MSCB. Contrary to the single-fan model of the MSCB, most foreland basins have rather complex topography, whereby slope processes, ponded sub-basin systems and other short-lived depositional systems are involved (Hiscott et al. 1986; Haughton 2001). Pulsating tectonic activity is thought to control the stratigraphic architecture of most foreland basins (Ricci-Lucchi 1986; Mutti and Normark 1987; Delvolvé et al. 1998; Ricken et al. 2000), whereas some deep-water foreland systems are controlled eustatically (Johnson et al. 2001). In this study we use an outcrop-scale facies analysis approach combined with ichnofacies analysis and sandstone and conglomerate provenance to resolve the contrasting lithologic and compositional features of the MF and to establish a dynamic facies model for this Variscan foreland basin system.

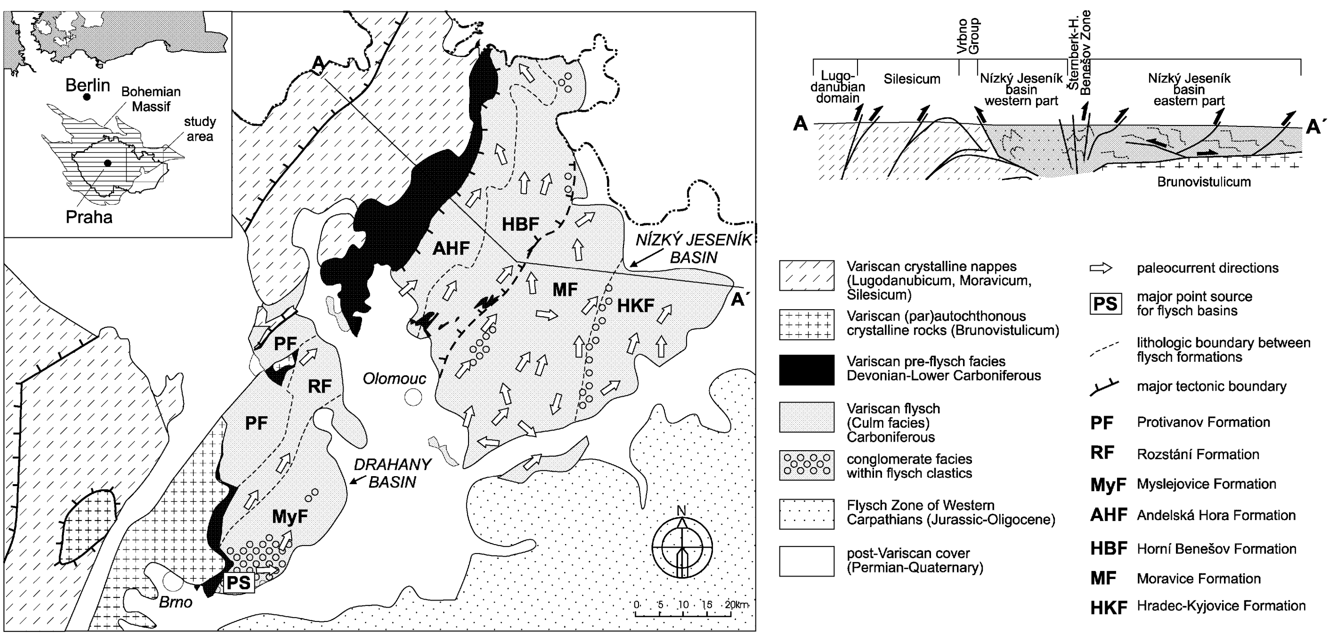

Fig. 2 Structure and principal features of the Moravo–Silesian Culm Basin in Moravia. Palaeocurrent data adopted from Kumpera and Martinec (1995), Schematic geological cross section modified according to Čížek and Tomek (1991) and Fritz and Neubauer (1995)

Geological setting and stratigraphy

The MSCB is preserved in an elongated structure trending SW–NE to SSW–NNE, bordered by Variscan crystalline nappes in the west (Schulmann et al. 1991) and by Tertiary to Quaternary deposits of the Carpathian Foredeep in the east (Fig. 2). The SW–NE to SSW–NNE trend corresponds to the overall structural trend at the eastern part of the Bohemian Massif resulting from Variscan dextral rotation of the Moravo–Silesian region due to oblique collision between the overriding Lugodanubian and subducting Brunovistulian terrane (Schulmann et al. 1991; Fritz and Neubauer 1995). The structure of the MSCB was interpreted as an E-directed imbricated fan of superficial flysch slices overlying the underplated Brunovistulian crystalline basement, together with its pre-flysch, Devonian to Lower Carboniferous sedimentary cover (Čížek and Tomek 1991). The MSCB shows a distinct W–E to NW–SE polarity in its deformation, metamorphosis and sediment composition. The intensity of deformation and metamorphic alteration generally decreases to the E to SE (Rajlich 1989; Franců et al. 2002). This trend continues further to the E to essentially undeformed Devonian to Lower Carboniferous strata covering the crystalline rocks of the Brunovistulian terrane, which is known from the subsurface. Similar, W–E to NW–SE polarity was observed in the sediment composition, from older, immature greywacke composition to younger, mature quartzose sandstone composition.

Lithostratigraphic subdivision of the Drahany and Nízký Jeseník Basins (Fig. 3) is adopted from Dvořák (1995) and Kumpera (1983). The Nízký Jeseník Basin was deposited in the Lower Viséan to lowermost Namurian interval and it is subdivided into four formations: Andělská Hora Fm, Horní Benešov Fm, Moravice Fm (MF) and Hradec—Kyjovice Fm. Three heavy-mineral zones were defined by Hartley and Otava (2001): (1) Lower Heavy Mineral Zone (Peγ Zone to base of Goα Zone) composed mainly of epidote, tourmaline, garnet, sphene and zircon; (2) Middle Heavy Mineral Zone with predominance of spessartine, grossular and almandine (base of Goα Zone to Goβ/Goγ Zone boundary); and (3) Upper Heavy Mineral Zone with predominance of pyrope and almandine (Goβ/Goγ Zone boundary to E1 Zone). The changes in heavy mineral spectra reflect an increasing proportion of high-grade metamorphics in the source area due to upper Viséan unroofing of high-grade metamorphic nappes of the Moldanubian terrane at approximately 330 Ma (Hartley and Otava 2001).

The MF is represented by about 1,800-m-thick succession of fine-grained turbiditic sandstones, siltstones and mudstones with minor proportion of thicker sandstone and conglomerate bodies (Kumpera 1983; Kumpera and Martinec 1995). The age of the MF is Upper Viséan (Goα2–3 to Goβmu Subzone) and the MF is subdivided into four informal units: Bohdanovice, Cvilín, Brumovice and Vikštejn Beds (Fig. 3). The whole MF falls within the Middle Heavy Mineral Zone of Hartley and Otava (2001).

Methodology

The study was focused on detailed measurement of 19 large outcrops aligned in two lines running roughly perpendicular to the mean strike, selected so as to represent two composite stratigraphic sections through the MF (Figs. 4 and 5), one reflecting the presumably more proximal facies in the previous submarine fan concept of Kumpera and Martinec (1995) and the other more distal ones. Measurement of sections was supported by semiquantitative analysis of trace fossil assemblages. In the provenance study we analysed medium- to coarse-grained sandstones and fine-grained conglomerates separately. The sandstone composition study was based on point counting of 34 uncovered thin sections from nine localities, with 300 grain counts per thin section, using the Gazzi-Dickinson method to minimize the variations due to different grain size (Ingersoll et al. 1984; Zuffa 1985). We used the grain classification scheme of Dickinson (1985); matrix and cement were not counted. The thin

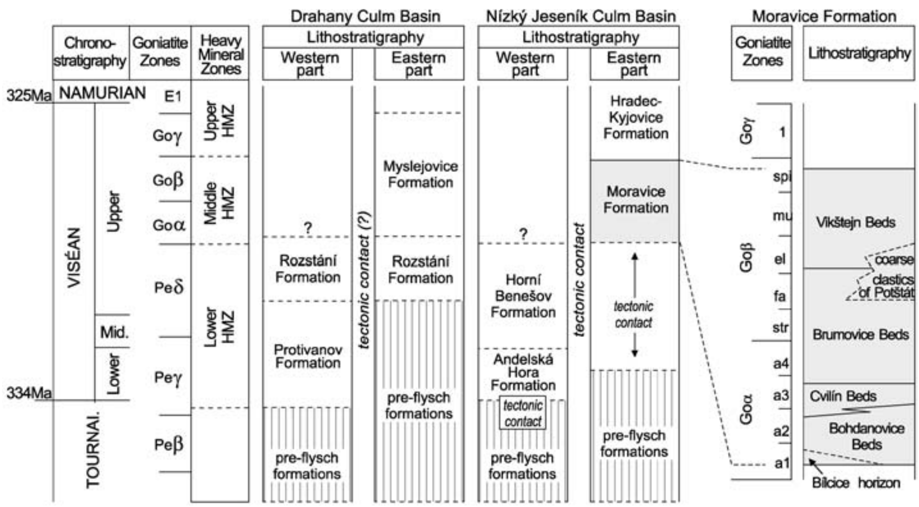

Fig. 3 Stratigraphy of the MSCB in Moravia. Modified from Kumpera (1983). Absolute boundary ages adopted from McKerrow and Van Staal (2000)

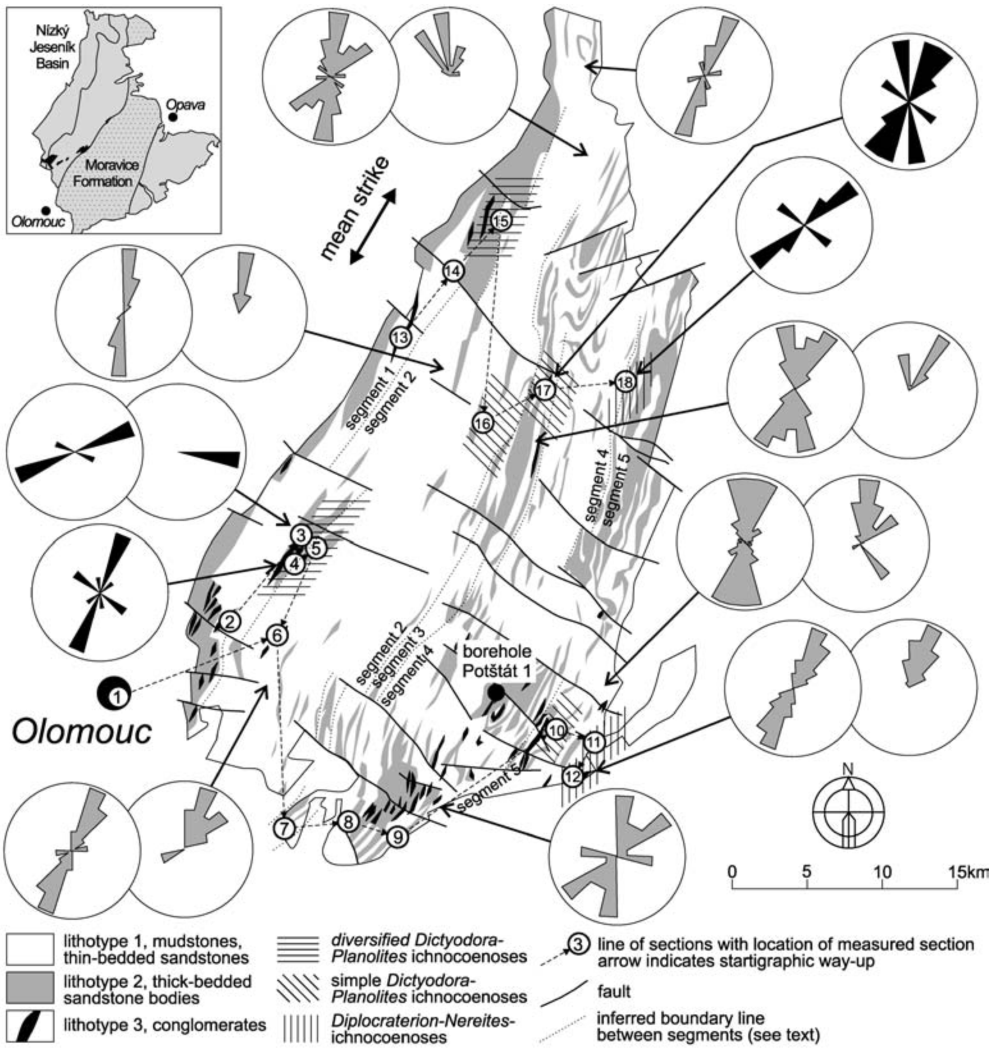

Fig. 4 Simplified geologic map of the MF showing distribution of basic lithotypes, composite section lines (*section numbers* correspond to those shown in Fig. 5), ichnocoenoses and palaeocurrent data. Palaeocurrent data (*grey diagrams*) adopted from Kumpera and Martinec (1995) and Hartley and Otava (2001). Our own palaeocurrent data are shown in *black diagrams*

sections were stained using the method of Houghton (1980) to allow for the discrimination of potassium feldspars and plagioclases. Study of fine-grained conglomerate composition was undertaken to trace more refined trends in lithic-grain composition than it is allowed by the Gazzi-Dickinson method alone (cf. Zuffa 1985; von Eynatten and Gaupp 1999). This study was based on point counting of 75 large thin sections from 15 localities (five analyses per locality), with 100 grain-counts per thin section.

Facies types and facies associations

Sandy debris flows

Beds of pebbly sandstones of facies type F2b are ungraded, have non-erosive bases and contain abundant outsized clasts (Table 1). The outsized clasts include both rounded extraclasts and plastically deformed intraclasts of thin-bedded turbiditic siltstones, mudstones and fine-grained sandstones. They are usually several dm to about 1 m long in α-axis diameter, but outsized clasts as long as 5 m were also found. The outsized clasts show random vertical distribution in the bed and they are not aligned in any discrete levels. Absence of bedforms, non-erosive nature and abundance of outsized clasts indicate these beds being deposited by friction freezing from non-turbulent, high-concentration density flows (Shanmugam 1996; Mulder and Alexander 2001). Most likely, these beds were not deposited from cohesive debris flows as their clay content is very low to zero (macroscopic observation) and no clast projection typical of cohesive debris flows is visible in them (cf. Hiscott and James 1985). The overall bed characteristics of this facies type

Fig. 5 Vertical stacking patterns of turbidite facies in selected measured sections (*left part*) and inferred, equal-thickness vertical distribution of measured sections in the northern and southern composite section of the MF (*right block*). *Numbered circles* = section numbers (see Fig. 4); *FA codes* = facies associations (see Table 2); *IC codes* = ichnocoenoses (see Table 3). See text for explanation of depositional systems, stratigraphic segments and megacycles

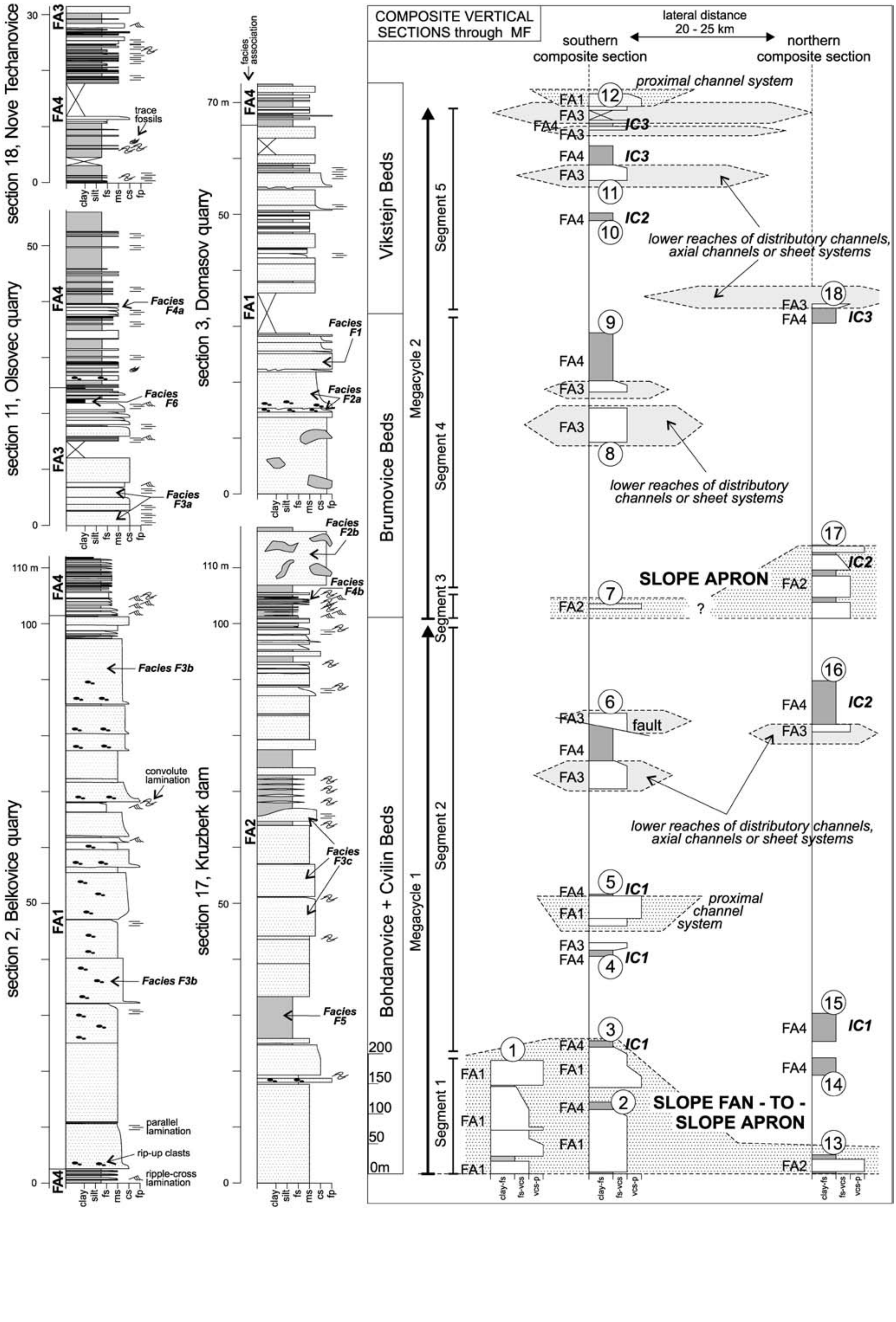
section 18, Nove Techanovice
section 11, Olsovec quarry
section 2, Belkovice quarry
section 3, Domasov quarry
section 17, Kruzberk dam
facies association
trace fossils
Facies F4a
Facies F6
Facies F3a
Facies F1
Facies F2a
Facies F2b
Facies F4b
Facies F3b
Facies F3c
Facies F5
convolute lamination
parallel lamination
rip-up clasts
ripple-cross lamination
clay silt fs ms cs fp
COMPOSITE VERTICAL SECTIONS through MF
lateral distance 20 - 25 km
southern composite section
northern composite section
Vikstejn Beds
Brumovice Beds
Bohdanovice + Cvilin Beds
Megacycle 1
Megacycle 2
Segment 1
Segment 2
Segment 3
Segment 4
Segment 5
proximal channel system
lower reaches of distributory channels, axial channels or sheet systems
lower reaches of distributory channels or sheet systems
SLOPE APRON
SLOPE FAN - TO - SLOPE APRON
fault
IC1
IC2
IC3
clay-fs fs-vcs vcs-p

suggest deposition from cohesionless, sandy debris flows (Shanmugam 1996; Falk and Dorsey 1998).

High-density turbidity current deposits

Clast-supported conglomerates with sandy matrix (facies type F1) and pebbly sandstones of facies type F2a are normally graded (Table 1). Both the facies types are thought to be deposited from high-density turbidity currents (Lowe 1982) as their normal grading indicates suspension settling and as a high flow concentration is required for transport and deposition of sediment particles larger than coarse sand (Middleton and Hampton 1973; Lowe 1982; Mulder and Alexander 2001). In contrast to the typical features of cohesive debris-flows, the beds of the facies type F1 sometimes have basal erosive scours, flat upper bed contacts (cf. Plink-Björklund et al. 2001) and low to zero content of clay matrix (cf. Mulder and Alexander 2001). Most beds of the facies type F1 correspond to the R_3 beds of Lowe (1982). In several beds of the facies type F1 there is a basal massive layer sometimes showing clast imbrication, which is followed by the normally graded conglomerate layer. This sequence suggests flow transformation from a basal layer deposited by friction freezing from non-turbulent hyperconcentrated flow (cf. Sohn 2001) to an upper layer deposited by suspension settling from concentrated (high-density) turbidity flow (the R_3 division). High-density flows that deposited the pebbly sandstones of facies type F2a were highly erosive as suggested by abundant basal scours (Fig. 6A) and mud intraclasts distributed near bed bases (Table 1). The beds show abrupt grain size jumps (Fig. 6B) from basal pebbly sandstone layer (the R_3 division) to upper, usually a parallel-stratified sandstone layer (S_1 of Lowe 1982). Sandstone beds of facies type F3a have a thick (up to 4 m), often normally graded and/or parallel stratified interval of coarse-grained sandstone, which is usually overlain by a relatively very thin Tb,c,d Bouma sequence (up to 30 cm). The normal grading, basal and internal scours and coarse sand lithology in the basal interval indicate deposition from turbulent density flows and this facies type can be classified as deposited from sand-dominated high-density turbidity currents (the S_1 and S_3 divisions of Lowe 1982, concentrated flows of Mulder and Alexander 2001). High erosive efficiency of these flows is indicated by abundant mud intraclasts distributed near bed bases and frequent basal scours.

Beds of the facies type F3b share similar succession of sedimentary structures with the facies type F3a and can thus be interpreted as high-density sandy turbidites. However, individual beds are very thick (usually about 8 to 10 m, occasionally up to 15 m) and show frequent traces of amalgamation such as internal scours and rip-up clasts (cf. Plink-Björklund et al. 2001; Mattern 2002) distributed in discontinuous layers in variable heights above bed bases. The facies type F3b is therefore assumed to represent amalgamated layers consisting of several high-density turbidite beds.

Quasi-steady turbidity current deposits

Up to 17-m-thick layers of medium grained sandstone of facies type F3c are non-erosive and structureless, except for occasional low-angle cross stratification and occasional faint normal grading and convolute lamination in the topmost parts of most beds. The layers are unusually thick but they do not show any traces of amalgamation and, therefore, each one probably represents a single depositional event. Great bed thickness is a feature typical of contained (ponded) turbidites, but thick mudstone intervals and upper-flow regime bedforms usually associated with contained deposits (cf. Pickering and Hiscott 1985; Haughton 2001) are not present in the beds of facies type F3c. Lateral pinch-out bed geometry was observed in one of the beds of facies type F3c (Fig. 6C). Absence of grading and great bed thickness may indicate deposition from quasi-steady hyperpycnal flows that may owe their origin to fluvial discharge (Kneller and Branney 1995), whereas surges and surge-like turbidity flows, unless ponded, do not produce thick sediment layers (Rothwell et al. 1992). The presence of cross stratification is in contradiction to sandy debris flow interpretation as such stratification forms solely beneath turbulent traction flows (Hickson and Lowe 2002, p. 349). Many examples of hyperpycnal flows are known from modern submarine fans (e.g. Kneller and Branney 1995; Mulder et al. 2001) and the occurrence of such deposits is probably underestimated in the fossil record, partly due to the difficulties with recognition of such flows from the bed characteristics (Kneller and Buckee 2000). Convex-upward shape and lateral pinch-out geometry of the beds of facies type F3c can be attributed to deceleration of the hyperpycnal current, loss of momentum and rapid deposition associated with a decrease in slope gradient (hydraulic jump).

Low-density turbidity current deposits

Heterolithic sandstone-siltstone-mudstone beds of the facies types F4a and F4b have usually sheet-like geometry (Fig. 6D) and they are organized into well-developed, complete or incomplete Bouma sequences. Frequent basal erosion marks and Ta,b,c,d Bouma sequences present in the facies type F4a suggest deposition from low-density turbidity currents (Middleton and Hampton 1973). The well-developed succession of bedforms expressed in the Bouma sequence indicate a progressive decrease in flow regime and an increase in traction during flow passage (Walker 1965), i.e. the features typical of surges or surge-like flows (Normark and Piper 1991; Kneller and Buckee 2000). Base-cut-out Tb,c,d Bouma sequences and predominant fine- to medium-grained sandstone lithology represent the typical features of the facies type F4b. Prevalence of upper-flow regime traction structures and relatively great thickness of individual beds (several dm to 1 m) suggest deposition from thick, low velocity turbidity flows, possibly in an channel overbank settings (cf. Leverenz 2000).

Table 1 Description of gravity-flow facies of the Moravice Formation

Facies type	Lithology	Sedimentary structures	Bed thickness	Bed contacts, bed geometry	Intraclasts, outsized extra-clasts	Depositional process
F1	Clast-supported conglomerate	Normally graded, sometimes massive in lower parts of beds, occasional clast imbrication near bed bases	2–13 m	Sometimes basal scours, flat upper contacts, bed geometry unknown	Very rare intraclasts, max. size 10 cm	High-density turbidity currents
F2a	Pebbly sandstone	Normally graded, sometimes parallel-stratified, grain-size jumps from basal pebbly sandstone division to upper sandstone division, internal scours	2–4 m	Frequent basal scours, flat upper contacts, bed geometry unknown	Abundant mud intraclasts distributed near bed bases, max. size 40 cm	High-density turbidity currents
F2b	Pebbly sandstone	Massive	8–12 m	Non-erosive basal contacts, flat upper contacts, bed geometry unknown	Abundant intraclasts and outsized extraclasts distributed throughout the bed thickness, max. size 500 cm	Sandy debris flows
F3a	Sandstone	Normally graded or massive, parallel-stratified, internal scours, Tb,c,d Bouma sequences near bed tops	1–4 m	Erosive basal contacts, flat upper contacts, bed geometry unknown	Sometimes mud intraclasts distributed near bed bases, max. size 15 cm	High-density turbidity currents
F3b	Sandstone	Massive, normally graded, sometimes coarse-tail graded, rarely inversely graded near bed bases, sometimes parallel-stratified, internal scours, Tb,c,d Bouma sequences near bed tops	3–15 m	Erosive basal contacts, flat upper contacts, bed geometry unknown	Abundant mud intraclasts distributed in bed-parallel or irregular zones in variable height above bed base, max. size 50 cm	Amalgamation of high-density turbidity current deposits
F3c	Sandstone	Massive, near bed tops faintly normally graded, convolute-laminated, parallel laminated or low-angle cross-laminated	1.5–17 m	Flat, non-erosive basal contacts, sometimes lateral pinch-out geometry, concave-up upper contacts		Quasi-steady turbidity currents
F4a	Sandstone to mudstone	Ta,b,c,d Bouma sequences, sometimes massive	Several cm to 1 m	Abundant tool marks and flute casts, sheet-like bed geometry		Low-density turbidity currents
F4b	Sandstone to mudstone	Tb,c,d (base-cut-out) Bouma sequences, frequently convolute-laminated	Several cm to ca. 50 cm	Non-erosive, flat bed bases, wavy tops		Low-density turbidity currents
F5	Siltstone to mudstone, rarely fine-grained sandstone	Normally graded, parallel laminated, ripple-cross laminated, low-angle cross-laminated	Several mm to 20 cm	Basal scours, load casts (load balls), flame structures, wavy tops, lateral pinch-outs of basal siltstone layers		Low-density turbidity currents
F6	Mudstone, rare siltstone	Faintly parallel laminated, sometimes bioturbated	Several cm to several dm			Hemipelagic fall-out, low-density turbidity currents

Fig. 6 Outcrop examples of turbidite facies from the MF. **A** Erosive scour at the base of high-density turbidite bed, facies F2a, section 5, Malý Rabštejn, Bohdanovice Beds; **B** graded bed of a high-density turbidite, conglomerate bed with a layer of floating clasts (traction carpet) near the base (upper tip of hammer) and a grain size jump into upper sandstone layer, facies F1, section 12, Hrabůvka quarry, Vikštejn Beds; **C** thick beds of quasi-steady turbidity current deposits interbedded with mudstone-siltstone intervals, note lateral pinch out and positive relief in the bed at the centre of photograph, facies F3c, section 17, Kružberk, Brumovice Beds, man for scale; **D** sheet-like beds of low-density turbidites, facies F4a, F5, section 16, Budišov nad Budišovkou, Cvilín Beds, *lens cap for scale* (right centre); **E** heterolithic siltstone-mudstone beds with sharp bases, initial load casts, parallel lamination and cross lamination, note lateral pinch-outs (bottom), facies F5, section 12, Hrabůvka quarry, Vikštejn Beds

Heterolithic siltstone-mudstone beds of facies type F5 (Fig. 6E) have typically an erosive base, a thin (0.5–3 cm), parallel laminated, ripple-cross laminated and/or normally graded siltstone layer showing frequent lateral pinch-outs, and a thick, sometimes bioturbated, upper mudstone layer (Table 1). Bed bases are sharp, commonly highly irregular due to scouring and loading of basal siltstone layers into the underlying mudstone. The extreme loading sometimes results in formation of detached load balls. The vertical succession of bedforms, low silt-clay ratio and loading features indicate these sediments to be qualified as fine-grained or silt turbidites with Bouma AE division (Shanmugam 1980; Piper and Stow 1991), deposited from low-density turbidity currents. Thick successions of more-or-less regular zebra-type alternation of the beds of facies type F5 were previously referred to as the “laminite” in the literature (Lombard 1963; Kumpera 1983) and they occur ubiquitously all over the MSCB. For the major part, these successions cannot be interpreted as bottom current deposits (contourites) due to the frequent erosive bases, normal grading and load casts present in the individual beds (Stow 1979).

Deep-water mudstones

Massive black mudstones of facies type F6, sometimes with thin silt laminae or bioturbated are very rare in the Moravice Formation. These deposits are difficult to interpret. Due to their common occurrence with silt turbidites (F5a) it is possible to interpret these deposits as base-cut-out silt turbidites or mud turbidites (Piper and Stow 1991). Alternatively, the mudstones may represent hemipelagic deposits of hypopycnal plumes associated with river discharge.

FACIES associations and facies stacking patterns

Because of its strong thrust-and-fold deformation, poor exposure and scarcity of stratigraphic markers the MSCB is almost impossible to interpret in terms of facies mapping based on lateral section correlation. It is, however, possible to link essentially incoherent outcrop-scale observations (cf. Leverenz 2000) to the regional scale using the general geological map of the MF, which shows a certain degree of lateral stratigraphic coherence. Three principal lithotypes have been determined in the geological map: (1) lithotype 1, thin-bedded, fine-grained sandstones, siltstones and mudstones, which are correlatable with the facies types F4a, F4b, F5 and F6; (2) lithotype 2, thick-bedded, medium- to coarse-grained sandstones corresponding to the facies types F3a, F3b, F3c and partly also F2a and F2b; and (3) lithotype 3, conglomerates corresponding to the facies type F1, and partly also F2a and F2b (Fig. 4). Interpretation of the measured sections reveals the MF to consist of four basic facies associations, which can be traced laterally in the regional scale using the geologic map: (1) FA1, channel fill deposits; (2) FA2, slope apron deposits; (3) FA3, lenticular sandstone bodies; and (4) FA4, fine-grained turbidites (Table 2).

FA1: channel fill deposits

The facies association 1 comprises high-density turbidites (F1, F2a, F3a, F3b) interbedded with minor low-density turbidites (F4a, F4b, F5) and occasional sandy debris-flows (F2b). In the map scale this facies association is exposed in lenticular units of the lithotype 2 and 3. In outcrop, the facies types are usually vertically stacked to form several tens of metres thick blocky cycles (Surlyk 1987) or thinning and fining upward (FU) cycles (Fig. 5, sects. 2, 3), sometimes consisting of higher-order, metre-scale FU cycles. Although FU cycles are characteristic features of turbidite systems in general and may occur both in confined and unconfined turbidite successions (Mutti 1992), such cycles have been mostly interpreted as filling confined channel forms and reflecting channel progressive abandonment, migration or upslope filling (Bouma et al. 1985; Mutti 1992; Pickering et al. 2001; Hickson and Lowe 2002). Similarly, blocky cycles

Table 2 Basic characteristics of facies associations of the Moravice Formation and their inferred depositional setting. Thickness and lateral continuity data estimated from the geological map

Facies association	Facies types	Stacking patterns	Thickness (m)/lateral continuity (m)	Depositional processes, depositional setting
FA1, channel-fill deposits	F1, F2a, F3a, F3b, more rarely F2b, F4a, F4b, F5	Asymmetric FU cycles, blocky cycles	Several tens to about one hundred metres/several hundred metres to first kilometres	Major, relatively proximal channels
FA2, slope-apron deposits	F2b, F3c, more rarely F3a, F4a, F4b, F5	Random facies distribution, blocky cycles, asymmetric FU cycles	Individual beds and cycles several tens of metres thick/several hundred metres to several kilometres	Slope apron, minor channels, individual debris-flows
FA3, lenticular, coarse-grained sandstone bodies	F3a, F3c, more rarely F3b, F4a, F5a	Partly unknown, gradual FU transitions in top parts, rare CU trends in lower parts	Several tens of metres/several hundred metres to several kilometres	Channel-lobe transitions, axial channels and/or unconfined sandstone lobes
FA4, fine-grained turbidite packets	F4a, F4b, F5, F6	Random vertical facies distribution	Several metres to several hundred metres/up to several tens of kilometres	Channel overbank settings, fringes of unconfined sandstone sheets, basin plain

indicate channel migration or channel abandonment (Surlyk 1987). Deposits of the FA1 show abundant basal and internal scours, mud intraclasts and frequent amalgamation, all of which imply high erosive competence of the flows. Abundance of amalgamation surfaces and average bed thickness is higher in channel areas than in unconfined sheet systems (cf. Carlson and Grotzinger 2001; Mattern 2002) and frequent erosion features are usually associated with channels or submarine canyons (Cavazza and DeCelles 1993; Ciner et al. 1996; Plink-Björklund et al. 2001). Despite the lack of information about their lateral pinch-out geometry, the sediments of the FA1 are thought to represent deposits of relatively proximal channel forms based on their overall coarse-grained lithology, stacking patterns and erosional features. In addition, a certain degree of lateral pinch-out geometry is suggested by lenticular shape of conglomerate and sandstone units of the lithotype 2 and 3 associated with the FA1 at the map scale. Facies characteristics suggest that most of the channels represent erosional or mixed erosional-depositional channels (Mutti and Normark 1987; Johnson et al. 2001).

FA2: slope apron deposits

The facies association 2 consists of quasi-steady turbidity current deposits (F3c) interbedded with low-density turbidity currents (F4a, F4b, F5) and occasional sandy debris flows (F2b). In the map this facies association is associated with thin units of the lithotype 2, showing lateral continuity over more than 10 km. In outcrop the facies types are vertically stacked to form about 15- to 40-m-thick blocky or fining upward units separated by metre-scale thick, mudstone-dominated units (Fig. 5, sect. 17). The individual sandy debris flows are vertically separated by the mudstone-dominated units and do not show vertical coherence with other sandstone units, arguing against a channel deposition. Thicker mudstone-dominated successions and the presence of sandy debris flows and their distribution in form of laterally incoherent bodies have been reported indicating slope or base-of-slope deposition (cf. Shanmugam and Moiola 1995). Similarly, deposits of quasi-steady turbidity currents have been reported from slope apron settings (Plink-Björklund et al. 2001) or indicating a close link to shelf-edge river systems (Sinclair 2000; Mulder et al. 2001). The blocky cycle and FU cycle organization of these deposits in the facies association 2 reflects filling of smaller-scale channels probably connected to a shelf-edge river system. Unusually high bed thickness and pinch-out geometry of the quasi-steady turbidity current deposits of F3c (see above) may reflect deposition in settings with significant decrease in bathymetric gradient, where the turbidity currents underwent hydraulic jumps (cf. Mutti and Normark 1987; Weimer et al. 1998). Deposition in lower reaches of a slope apron setting or in a topographically complex slope setting (slope basins) is inferred for the FA2.

FA3: lenticular, coarse-grained sandstone bodies

The facies association 3 is composed of high-density turbidite sandstones (F3a, F3b) interbedded with quasi-steady flow turbidites (F3c) and low-density turbidites (F4a, F4b, F5). In the map scale, this facies association is distributed either in lenticular or in laterally continuous units of the lithotype 2. In outcrop, the facies types usually show several tens of metres thick fining upward successions from the FA3 to FA4 (below) in their upper parts (Fig. 5, sect. 11), whereas their basal parts are usually not exposed except for the section 19, in which a coarsening-upward trend from FA4 (see below) to the basal part of the FA3 was observed (Fig. 5, sect. 18). Relative lower proportion of amalgamation surfaces, lower average bed thickness, scarcity and generally small size of mudstone intraclasts and absence of internal asymmetric FU cycles provide the criteria to distinguish the FA3 from the typical channel fill deposits of the FA1 association. It is, however, difficult to interpret the FA3 as typical sandstone lobe deposits. Compared with channelized systems, a typical sandstone lobe system is usually associated with metre-scale thick sandstone compensation cycles (Mutti and Sonnino 1981), good correlation between grain size and bed thickness, indicating attainment of flow equilibrium and longer transport (Leverenz 2000), and higher proportion of sheet-like beds with well-developed complete Bouma sequences and tool marks (Ciner et al. 1996). In the FA3, the example of the basal CU trend may indicate sandstone lobe progradation (Mutti and Ricci-Lucchi 1975; Shanmugam and Moiola 1985), but, in general, the proportion of sandstone beds with Bouma sequences is usually low, internal compensation cycles were not found and there is a very high proportion of thick, coarse-grained beds of high-density turbidites (F3a, F3b) relative to low-density ones. Most probably, the FA3 may indicate deposition in the lower reaches of distributory channels or in channel-lobe transitions (Mutti and Normark 1987). Alternatively, the FA3 may represent axial channel fills, which is supported by the basin axis-parallel palaeocurrent directions (cf. Lewis and Barnes 1999; Leverenz 2000). Similarly, Hartley and Otava (2001) have reported from the MSCB the bundles of high-density turbidite sandstones showing similar facies characteristics and sheet-like geometry traceable over 150 m, interpreting them as unconfined sandstone sheets (lobes) or fills of shallow channels. Closer interpretation is probably difficult to attain due to the lack of more detailed information about bed geometry (cf. Plink-Björklund et al. 2001).

FA4: fine-grained turbidite packets

The association FA4 is composed essentially of low-density turbidity current deposits (F4a, F4b, F5) and deep-water mudstones (F6). In the map, the FA4 association comprises several tens to several hundred metres thick successions of the lithotype 3, punctuated by units of the

FA1, 2 and 3. Fining upward facies transitions from the FA1, FA2 and FA3 to the successions of the FA4 are most frequently visible in outcrop whereas the lower contacts show more complex patterns (see the discussion above).

Multiple ways in interpreting the depositional setting of the FA4 association are suggested including lobe fringe to basin plain and channel-overbank deposits. The FA4 association is partly composed of successions of thin, plane parallel beds of low-density sandy a silty turbidites, commonly with complete Bouma sequences (F5a) and abundant tool marks, showing random stacking patterns. Consistently with their facies characteristics, palaeocurrent patterns and deep-water trace fossils (see below) these successions are thought to represent products of distal turbidite system depositional settings (fringes of unconfined sandstone sheet bodies, basin plain, cf. Agirrezabala and García-Mondéjar 1994). On the other hand, thick successions of the zebra-type alternation of lenticular silt turbidites with abundant load casts, ripple-cross lamination and essentially no trace fossils (F5) indicate rapid particle fall-out probably associated with expansion of high-energy flows in a channel levee environment or in channel-termination areas (Piper and Stow 1991; Cavazza and DeCelles 1993). In several outcrop examples, the fining upward transitions from the FA1 or FA3 associations to the FA4 association are emphasized by metre-scale or several tens of metres-thick successions of fine-grained sandstones with base-cut-out Bouma sequences (F4b). Frequent convolute lamination present in the facies type F4b suggests rapid suspension settling and water escape, which may be associated with deposition in proximal, high-energy channel-overbank environments (Hickson and Lowe 2002). The channel-overbank interpretation, however, is not conclusive as direct lateral transitions from channels to levees were not observed and, in general, levee facies are difficult to distinguish based solely on facies characteristics (cf. Ciner et al. 1996; Hickson and Lowe 2002). Further considerations including ichnofacies characteristics (see below) are required to achieve more precise environmental interpretation.

Palaeocurrent directions

Both unidirectional and bi-directional palaeocurrent data were obtained from the orientation of flute casts and tool marks, mostly from low-density turbidity current deposits (F4a, F5). The absolute majority of both published and our own palaeocurrent data indicate S–N to SW–NE directions of flow with SSW–NNE frequency maximum (Fig. 4). This direction has been assumed to be parallel to the basin depocentre axis (Kumpera 1983; Hartley and Otava 2001). Such palaeocurrent patterns are typical of the whole MSCB, indicating axial-trough topography at the time of deposition. A much smaller amount of the palaeocurrent indicators show alternate W–E and NW–SE directions, which are oblique to perpendicular to the basin axis. Especially in the basal parts of the Moravice Formation, the palaeoflow patterns are relatively more complex, showing a relatively higher proportion of the oblique to perpendicular W–E to NW–SE directions. In the upper parts of the MF the palaeoflow patterns are more uniform and tend to the SSW–NNE frequency maximum.

Trace fossils and ichnofacies

Compared with the older Culm formations in the MSCB, the sediments of the Moravice Formation contain relatively rich trace fossil assemblages, whose abundance and diversity generally increases towards its younger parts (Mikuláš et al. 2002). Trace fossils of the MF are being found purely in low-density turbidites (facies types F5, F4a, F4b) and deep-water mudstones (F6). Three types of ichnocoenoses were observed in the MF, each reflecting a distinct environmental control: (1) diversified Dictyodora–Planolites; (2) simple Dictyodora–Planolites; and (3) Diplocraterion–Nereites.

The diversified Dictyodora–Planolites ichnocoenosis (Table 3, Fig. 4) consists mostly of fodinichnia (feeding traces) accompanied by agrichnia, pascichnia (grazing traces) and traces showing complex feeding strategies, such as chemosymbiosis and gardening (*Chondrites, Dictyodora*). Traces such as *Phycosiphon* indicate deep-water, poorly oxygenated environments whereas *Zoophycos* have been reported both from shallow- and deep-water settings (Seilacher 1967; Pfeiffer 1969; Plička 1970; Wetzel and Werner 1981; Ekdale and Manson 1988). Similarly, *Planolites* represents an eurybathic, extremely facies-crossing form (Pemberton and Frey 1982; Fillion and Pickerill 1990). In the classical Seilacher's (1967) concept, this ichnocoenosis can be considered as a transitional Zoophycos–Nereites ichnofacies indicating typically bathyal, aphotic, low-energy, oxygen-depleted environments, which are unfavourable for the benthic communities to live and evolve (Frey and Pemberton 1984).

The simple Dictyodora–Planolites ichnocoenosis (Table 3, Fig. 4), despite its relatively high specimen abundance in the localities, shows extremely low diversity, comprising only two ichnogenera. Producers of these traces were sediment feeders developing specialized feeding strategies to make the best use of their low-nutrient level environments (Frey and Pemberton 1984). This ichnocoenosis can be assigned to the Nereites ichnofacies indicating deep-marine environment with extremely low energy levels (Frey and Pemberton 1984; Stepanek and Geyer 1989; Orr 2001). Traces of the Nereites ichnofacies have been reported from the Culm facies of Germany and England (Stepanek and Geyer 1989; Hofmann 1993). There are more-or-less gradual transitions between the diversified and the simple Dictyodora–Planolites ichnocoenoses, which manifest themselves in a gradual decrease in diversity of pascichnia and pascichnia–fodinichnia type traces from the former to the latter, whereas the diversity level of typical fodinichnia,

Table 3 Abundance of ichnogenera and ichnospecies per trace fossil locality, definition of ichnocoenoses and inferred ichnofacies according to Seilacher (1967); * 1–2 specimens; ** 3–6 specimens; *** 7–15 specimens; **** >15 specimens. Arrows between facies association codes (FA) indicate transitional beds between facies associations

Measured section no. (*N* = not measured)		3	4	5	N	15	16	17	10	18	11	12
Agrichnia	*Protopaleodictyon* isp.			*					*	**	**	
Agrichnia–pascichnia	*Cosmorhaphe* isp.									*	****	
	Cosmorhaphe timida		**	**						*	****	
	Furculosus isp.										**	
	Nereites isp.									***	****	
	Phycosiphon incertum		**	***								
	Urohelminthoida isp.										*	
Pascichnia	*Pilichnus* isp.	*										
	Zoophycos isp.		*									
Pascichnia–fodinichnia	*Chondrites* cf. *intricatus*				*							
	Chondrites isp.	*	**	**	*					**	**	
Fodinichnia	*Dictyodora liebeana*	***	****	****	***	****	***	***	****	****	****	***
	Falcichnites lophoctenoides	*										
	Laevicyclus isp.					**						
	Planolites beverleyensis	**	***	****	***	***	***	****	***	*		**
	Planolites isp.	**	****	****	***	****	***	**	***	*		**
Domichnia	*Diplocraterion* isp.									**	****	****
	Rhizocorallium isp.			*						**	****	****
Facies association		FA1 -> FA4	FA1 -> FA4	FA4	FA4	FA4	FA2	FA3 -> FA4	FA4	FA4 -> FA3	FA3 -> FA4	FA3 -> FA4
Ichnocoenosis (IC)		IC1, diversified: Dictyodora–Planolites					IC2, simple: Dictodora–Planolites			IC3: Diplocraterion–Nereites		
Ichnofacies interpretation		Zoophycos–Nereites					Nereites			Cruziana–Nereites		

such as *Dictyodora* and *Planolites*, remains almost constant.

The relatively highly diverse Diplocraterion–Nereites ichnoceonosis (Table 3, Fig. 4) comprises abundant domichnia (dwelling traces), fodinichnia and agrichnia-pascichnia type traces. In contrast to the previous ichnocoenoses, this one comprises abundant traces of suspension feeders or possible surface-scraping detritus feeders, such as the *Diplocraterion* (Fürsich 1974). Sea-floor colonization solely by suspension feeders is a common feature of the present-day poorly oxygenated bottoms (Rhoads and Boyer 1982). The ichnogeneric composition of this ichnocoenosis corresponds to the Cruziana ichnofacies mixed with traces of the Nereites ichnofacies sensu Seilacher (1967) and Frey and Pemberton (1984), and suggests deposition in environments more favourable to colonization compared with the previous ichnocoenoses. The nutrient levels and bottom oxygenation, as indicated by this ichnocoenosis, were the highest of all environments in the MF.

Sediment composition and provenance

The sandstones of the MF can be characterized as quartzolithic to quartzo-feldspathic sandstones with average concentrations $Q_{61}F_{26}L_{13}$ (see Table 4 for point-counting data). The modal composition corresponds to recycled orogen to transitional continental type of clastic provenance (Dickinson et al. 1983). Up-section, statistically significant shifts occur in grain concentrations of the MF (Figs. 7 and 8). In its lower part (Bohdanovice and Cvilín Beds, Goα1 to Goα2 Zone interval) concentrations of total unstable lithic grains (L) decrease whereas total feldspars (F) concentrations increase. At the same time, the Qm/Qp ratio increases from values <1.0 to ~1.0 (Fig. 8). Rapid increase in K-feldspar concentrations is detected at the base of the Brumovice Beds (Goα3/4) along with a gradual increase in the Qm/Qp ratio towards values >1.0 during the interval of deposition of the Brumovice Beds (Goα3/4 to Goβfa). In the same interval, total unstable lithic grains retain approximately uniform mean concentrations. Mean concentrations of feldspars decrease at the base of the Vikštejn Beds (Goβel) and during the interval of sedimentation of the Vikštejn Beds (Goβel to Goβspi) concentrations of total unstable lithic grains decrease, whereas the Qm/Qp ratio increases to reach the values of >2.0 in the upper parts of the beds (Fig. 8).

Up-section, conglomerates of the MF show significant shifts in the composition of their fine-grained conglomerate fraction (Fig. 7). In the lower part of the MF (Bohdanovice and Cvilín Beds, Goα1 to Goα2 Zone interval) clasts of sedimentary rocks (22 to 39%) predominate over quartz clasts, magmatic lithic clasts (21 to 24%) and metamorphic lithic clasts (11.5 to 20.5%). In the middle and upper part of the MF (Brumovice and Vikštejn Beds, Goα3/4 to Goβspi Zone interval) magmatic lithic clasts (28.5 to 47.5%) start to predominate

Table 4 Recalculated sandstone composition data from the MF. *BOHD* Bohdanovice Beds; *BRUM* Brumovice Beds; *VIK* Vikštejn Beds; *Qm* monocrystalline quartz; *Qp* polycrystalline quartz; *P* plagioclase feldspars; *K* potassium feldspars; *Lv* volcanic lithic clasts; *Lmet* metamorphic lithic clasts; *Ls* sedimentary lithic clasts; *L(indet)* undetermined lithic clasts; *Q* total quartz; *F* total feldspars; *L* total lithic clasts

Locality	Lithostratigraphy	Qm (%)	Qp (%)	P (%)	K (%)	Lv (%)	Lmet (%)	Ls (%)	L(indet.) (%)	Q (%)	F (%)	L (%)
Domašov 1	BOHD	24	37.5	2.5	4.5	0.5	18	5	8	61.5	7	31.5
Domašov 1	BOHD	25.5	39	3.5	11.5	0	10.5	4.5	5.5	64.5	15	20.5
Domašov 1	BOHD	23.4	37.1	4.1	12.2	0	14.2	4.1	5.1	60.5	16.3	23.4
Domašov 1	BOHD	27.5	35	4.5	11.5	0	11	4	6.5	62.5	16	21.5
Domašov 1	BOHD	28.5	28.5	7.5	21	0	10	3.5	1	57	28.5	14.5
Domašov 1	BOHD	39	39	3	7.5	0	6	3	2.5	78	10.5	11.5
Domašov 2	BOHD	31.7	37.1	5.4	9.4	0.5	7.9	2.5	5.4	68.8	14.8	16.3
Bělský mlýn 1	BOHD	24.4	35.2	9.3	13	0	13	3.6	1.6	59.6	22.3	18.2
Bělský mlýn 1	BOHD	46	14.5	8.5	20.5	0	6	2.5	2	60.5	29	10.5
Bělský mlýn 1	BOHD	26.5	24	4.5	30.5	0	7	4	3.5	50.5	35	14.5
Bělský mlýn 2	BOHD	36.5	38	5	8	0	6.5	2	4	74.5	13	12.5
Bělský mlýn 2	BOHD	31.3	46.4	4.2	7.3	0	5.2	1.6	4.2	77.7	11.5	11
Kružberk 1	BRUM	16.9	10.7	5	60.9	1.5	3.4	1.5	0	27.6	65.9	6.4
Kružberk 1	BRUM	28.9	15.4	7.7	40.7	0.4	2.6	4.4	0	44.3	48.4	7.4
Kružberk 1	BRUM	23.9	19.3	4.9	39.4	2.3	7.6	2.7	0	43.2	44.3	12.6
Kružberk 1	BRUM	30.8	25.1	5.3	30.8	0	6.1	1.9	0	55.9	36.1	8
Kružberk 1	BRUM	25.8	29.2	4.1	32.2	0.7	5.2	2.6	0	55	36.3	8.5
Skoky 1	BRUM	22.8	41.8	0.4	33.8	0	0.8	0.4	0	64.6	34.2	1.2
Skoky 1	BRUM	22.3	31	2.6	36.2	0	7.4	0.4	0	53.3	38.8	7.8
Skoky 1	BRUM	21.1	37.4	1.8	30.4	0	9.3	0	0	58.5	32.2	9.3
Těchanovice 1	BRUM	32.4	25.7	2.8	18.3	1.1	12.7	7	0	58.1	21.1	20.8
Těchanovice 1	BRUM	17	36.9	4.1	25.8	0.7	11.1	4.4	0	53.9	29.9	16.2
Těchanovice 1	BRUM	22.4	28.7	2.2	20.1	1.5	18.7	6.3	0	51.1	22.3	26.5
Těchanovice 1	BRUM	26.3	25.9	2.9	25.9	0	10.4	8.6	0	52.2	28.8	19
Olšovec 1	VIK	45.5	12.2	5.8	27	0	6.9	0.5	2.1	57.7	32.8	9.5
Olšovec 1	VIK	56	26	3.5	12	0	0.5	1.5	0.5	82	15.5	2.5
Olšovec 1	VIK	52	21.5	6.5	15	0	2.5	2	0.5	73.5	21.5	5
Olšovec 1	VIK	51.5	21.5	1.5	20.5	0.5	3.5	1	0	73	22	5
Olšovec 1	VIK	31	16	8.6	26.7	0	8	6.4	3.2	47	35.3	17.6
Hrabůvka 1	VIK	33.5	31	5.5	8.5	0	10	11.5	0	64.5	14	21.5
Hrabůvka 1	VIK	42.5	31.5	2.5	13.5	0	4.5	1	4.5	74	16	10
Hrabůvka 1	VIK	37	26	1.5	24.5	2.5	7	0	1.5	63	26	11
Hrabůvka 1	VIK	45.5	29	4.5	11.5	0	5.5	0.5	3.5	74.5	16	9.5
Hrabůvka 1	VIK	42.2	28.1	7.8	14.6	0	3.1	2.6	1.6	70.3	22.4	7.3

over sedimentary lithic clasts (14 to 27.5%), quartz clasts (10.5 to 32%) and metamorphic lithic clasts (13.5 to 25%). In addition, there is a noticeable increase in the ratio of plutonic to volcanic lithic clasts in the middle part of the MF relative to its lower part, from values generally <1.0 to values >1.0 to 2.0 (Fig. 7). Four localities were sampled in the overlying Hradec–Kyjovice Formation (Goβspi to Goγ) showing a significant positive shift in concentration of the quartz clasts (36 to 54%), whereas the concentration of magmatic (15 to 40%) and metamorphic lithic clasts (2 to 21%) generally decreases and the mean concentration of sedimentary lithic grains (5 to 34%) remains basically unchanged (Fig. 7).

The compositional data suggest the lower part of the MF to be derived mostly from mixed sedimentary- low-grade metamorphic-plutonic sources with minor proportion of volcanic sources (indicated mainly by potassium feldspars and polycrystalline quartz in the sandstones and volcanic and sedimentary lithic clasts in the conglomerates). The overall up-section increase in monocrystalline quartz grains in the sandstones can indicate increased supply from recycled sedimentary or metamorphic sources (von Eynatten and Gaupp 1999). However, conglomerate composition data show essentially no change in concentrations of sedimentary lithic grains, a decrease in concentrations of metamorphic lithic clasts and an increase in concentrations of magmatic lithic clasts and quartz clasts. Most probably, increasing proportion of sediment derived from high-grade metamorphic rocks and magmatic rocks up-section caused this trend, but other processes related to increasing sediment maturity such as weathering, coastal reworking, etc. may have been involved. Higher concentrations of potassium feldspars in sandstones in the Brumovice Beds relative to the older members may indicate either increased supply from plutonic sources or less intense weathering due to shorter residence times in fluvial and near-shore environments (cf. Fergusson and Tye 1999). The former is believed more likely as this trend is accompanied by the increase in the ratio of plutonic to volcanic lithic clasts in conglomerates. In general, there is an overall trend in the decreasing supply from volcanic/low-grade metamorphic sources and increasing supply from plutonic/high-grade metamorphic sources up-section, which can be attributed

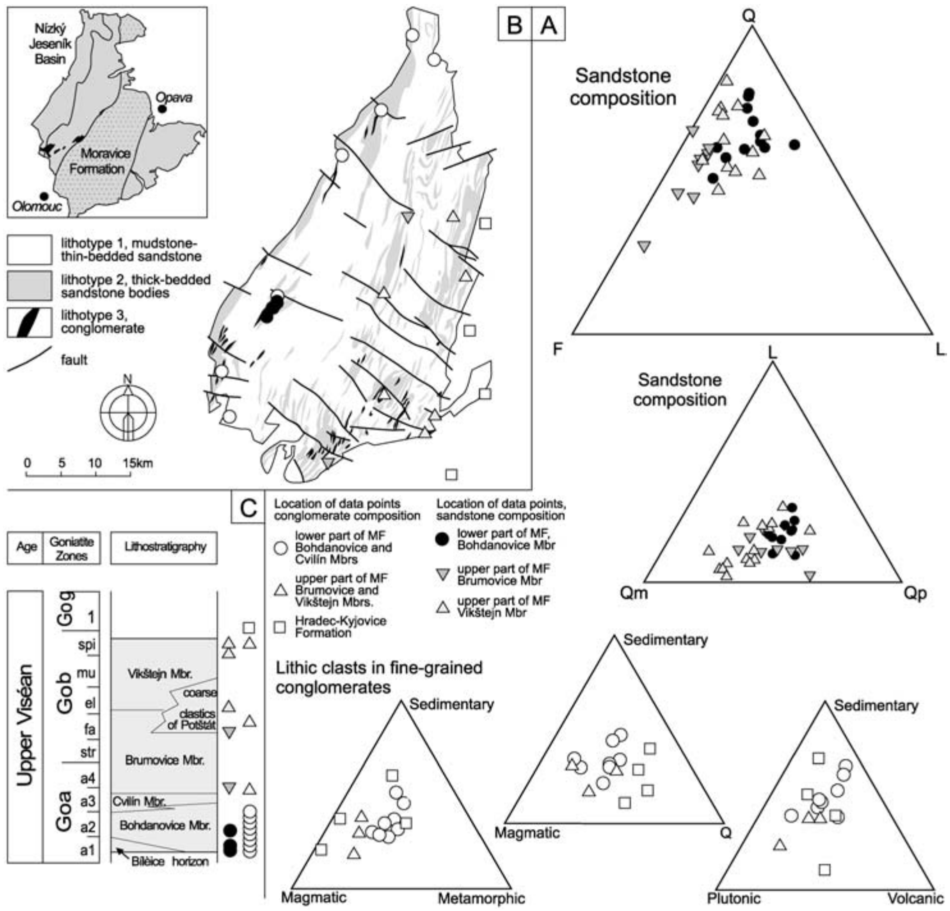

Fig. 7 **A** Ternary plots of sandstone and fine-grained conglomerate composition in the MF; **B**, **C** map and stratigraphic distribution of point-counted samples. Sandstone composition groups: *Q* total quartz clasts; *F* total feldspar clasts; *L* total lithic clasts; *Qm* monocrystalline quartz clasts; *Qp* polycrystalline quartz clasts

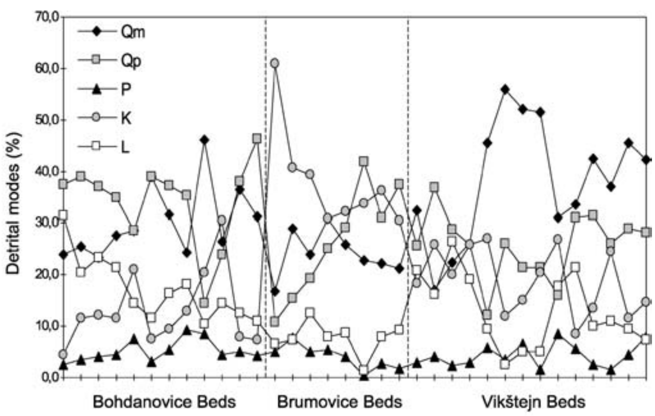

Fig. 8 Stratigraphic distribution of sandstone composition data. *Qm* monocrystalline quartz clasts; *Qp* polycrystalline quartz clasts; *P* plagioclase feldspars; *K* potassium feldspars; *L* total lithic clasts

to uplift in the source area and unroofing of its structurally deeper crustal parts (cf. Dorsey 1988; Critelli et al. 1995). This trend was accelerated with the onset of deposition of the Hradec–Kyjovice Formation approximately at the Goβ/Goγ Zone boundary (boundary between the Middle and Upper Heavy Mineral Zone). The sudden shift towards quartz-rich conglomerate compositions at this boundary is thought to reflect even more significant supply from high-grade metamorphic terrains. This is supported by the published heavy mineral spectra (Hartley and Otava 2001), in which high concentrations of pyrope and almandine suggest low sediment maturity and derivation from metamorphic sources. The same authors considered this compositional change to reflect a basin-wide progradation associated with sediment oversupply from the exhumed Moldanubian nappe pile at approximately 330 Ma.

Cyclic patterns in the Moravice formation

The deep-water facies in the MF show a distinct vertical arrangement, which is well constrained from the vertical distribution of facies associations, palaeocurrent patterns and trace fossils. Five distinct stratigraphic segments were recognized.

The basal segment 1 (Bohdanovice Beds, Goα1 to ~Goα2 Zone interval) is composed of about 200- to 250-m-thick successions of the erosive channel fills (FA1) and possibly overbank deposits (FA4) in the southern composite section (Fig. 5). In the northern composite section, their lateral equivalents are represented by thinner slope apron deposits with occasional sandy debris-flows (FA2, Fig. 5). Palaeocurrent measurements indicate a predominant SSW–NNE, basin axis-parallel sediment dispersal, but there is a relatively high proportion of the perpendicular W–E and NW–SE palaeocurrent directions (Fig. 4, see also Kumpera 1983). Considering its rather coarse-grained channel-fill nature, scarcity of well-defined lobes and presence of the bathyal Zoophycos–Nereites-type trace fossils we suggest that this succession was deposited in proximal, channel-dominated parts of a low- to moderate-efficiency turbidite system of type II to type III (Mutti and Normark 1987; Emery and Myers 1996). As suggested by the facies distribution in the map and the palaeocurrent directions, the system was largely supplied from a linear source or multiple point sources (cf. Reading and Richards 1994) located west of the depositional locus (in the present-day orientation).

The basal segment is overlain by about 550- to 750-m-thick segment 2 composed of fine-grained turbidites (FA4, Fig. 5) with infrequent erosive channels (FA1, section 5) and few isolated sandstone bodies (FA3) deposited in channel-lobe transitions, axial channels or in sandstone lobes. The segment 2 corresponds to the upper parts of Bohdanovice Beds and Cvilín Beds (~Goα1 to Goα2 Zone interval). The generally fine-grained nature, high sedimentation rates (see below), scarcity of erosive channels and presence of trace fossils of the Nereites ichnofacies, which is thought to represent the lowest energy environments within the whole MF, suggest the segment 2 represents distal parts of a rather high-efficiency turbidite system (Mutti and Normark 1987). The great majority of palaeocurrent data are parallel to subparallel to the SSW–NNE basin axis (Fig. 4), indicating a predominant northward dispersal, probably from a point source located in the (present-day) south (cf. Kumpera and Martinec 1995; Hartley and Otava 2001).

The overlying segment 3 (Fig. 5) is represented by a relatively thin succession of fine-grained turbidites, sandy debris flows, minor channel-fills and thick, quasi-steady turbidity current deposits (FA3). The segment 3 corresponds to the basal part of the Brumovice Beds (~Goα3/4) and it can be traced laterally from the northern composite section (about 150 m thick) down to the southern composite section (about 50 m thick). Trace fossils of the Nereites ichnofacies indicate very low-energy, poorly oxygenated environments. Palaeocurrent data indicate predominant basin axis-parallel sediment dispersal and a very subordinate dispersal perpendicular to the basin axis. This segment is interpreted as mixed sand-mud slope apron (Reading and Richards 1994) or as a fill of minor slope basin (see discussion above).

The overlying segment 4 is about 400 m thick and it corresponds to the upper part of the Brumovice Beds (~Goβstr to Goβfa Zone). In the northern composite section it is composed mostly of fine-grained turbidites (FA4) intercalated with isolated bodies of lenticular sandstones (FA3) interpreted as channel-lobe transition deposits, lobes or axial channel fills (Fig. 5). Palaeocurrent data, facies characteristics and sedimentation rates are similar to those of the segment 2 (~Goα1 to Goα2 Zone interval) and suggest deposition in distal parts of a rather high-efficiency turbidite system with S to N sediment dispersal. In the southern section of the same segment the fine-grained turbidites are intercalated with hundred metre-thick multi-storey lenticular sandstones (FA3). Map distribution of the lithotypes associated with the sandstones in the southern section indicates that there are several vertically stacked FA3 sandstone bodies with a rather limited lateral extent (Fig. 4), alternating with minor fine-grained turbidites. This suggests a point source-fan geometry rather than axial channel or sheet geometry, which is also supported by rather diverse palaeocurrent directions associated with the FA3. These deposits are thought to represent channel-lobe transitions of a relatively small, point-sourced, sand-rich, low-efficiency turbidite fan (Mutti and Normark 1987; Reading and Richards 1994).

The uppermost segment 5 is about 300 m thick, sand-rich and corresponds to the Vikštejn Beds (Goβel to Goβspi). This succession is mostly composed of sandstone bodies of the FA3 alternating with fine-grained turbidites of the FA4 (Fig. 5). In the map, the sandstone bodies can be traced laterally for more than 10 km (Fig. 4). The relatively diverse trace fossil assemblages of the Nereites–Cruziana ichnofacies occur for the first time in this segment. Presence of domichnia of the Diplocraterion and Arenicolites type in deep-sea fan sediments have been considered to reflect local conditions such as relative high energy setting, sandy substrates and relative good oxygenation (Buatois and Angriman 1992; Mutti 1992). Trace fossils of the Cruziana ichnofacies are not known from older sand-rich horizons within the MSCB and, consequently, their first occurrence in the uppermost segment is considered to reflect a regional-scale change in the basin topographic configuration (uplift, oversupply) rather than simple shifts of local depositional settings. Palaeocurrent data indicate prevailing northward, axial sediment dispersal with minor eastward transport directions. The uppermost segment most probably represents deposition of laterally coalescent, transitional channel-lobe sandstones or lobe sandstones in a relative sand-rich turbidite system (Reading and Richards 1994).

Discussion: possible controls on the cyclic deposition

The MF shows a distinct cyclic alternation of proximal turbidite systems to slope systems (segments 1 and 3) and distal turbidite systems (segments 2 and 4). The segment 5 represents an excursion from this cyclicity, which is probably related to a reconfiguration of the basin as a whole (see below). The segments 1 and 3 consist of proximal, erosive channel-dominated, low-efficiency turbidite systems and slope-aprons. The basal, erosive channels of the segment 1 are sharply separated from the underlying fine-grained deposits (Fig. 5, section 2). This vertical arrangement is included in most of the seismic-based sequence stratigraphic models (Posamentier and Vail 1988; Posamentier et al. 1991; Kolla 1993) where it indicates a depositional sequence boundary overlain by a lowstand fan in the up-dip sections. The same interpretation is also supported by outcrop data with well-constrained sequence stratigraphic framework (Johnson et al. 2001). Basal erosive (sequence) boundary was not observed in the segment 3, but the deposition of sandy debris flows and quasi-steady turbidity currents are usually thought to indicate relative sea-level lowstands, the latter being related to direct river discharge to the basin (Normark et al. 1998; Plink-Björklund et al. 2001). In this respect, segment 3 is comparable to segment 1 and both are considered to represent lowstand turbidite systems bounded by basal sequence boundary. Upper parts of segments 1 and 3 show relatively gradual vertical transition into the distal, high-efficiency, fine-grained turbidite systems of segments 2 and 4, which probably indicate relative sea-level highstand (Normark et al. 1998). We consider the cyclic alternation of segments to represent two asymmetric megacycles, each bounded by a basal sequence boundary and comprising a basal lowstand turbidite system (segments 1 and 3) and an upper highstand turbidite system (segments 2 and 4).

Cyclic arrangement of turbidite systems is a characteristic feature of most deep-water foreland basins and the cycles have been attributed to different control mechanisms (see below).

Eustatic sea-level cycles can be documented to provide the major control on stratigraphic evolution of deep-water siliciclastics in otherwise tectonically active settings, provided that the timing of stratigraphic cyclicity fits the available eustatic curves. Examples of eustatically driven deep-water systems include Ordovician Taconic foreland basin in Canada (Hiscott et al. 1986), Permian Karoo Basin in South Africa (Johnson et al. 2001) and Miocene Pohang back-arc basin in South Korea (Sohn et al. 2001). Lower Carboniferous global eustatic cycles are well constrained from cratonic onlap studies (Ross and Ross 1985). Eight global eustatic cycles, each with a 100- to 200-m amplitude, were recognized in the Viséan period. In the MF, basal segments of the megacycle 1 (Goα1 to ~Goα2 Zone interval) and megacycle 2 (~Goα3/4 Zone) correspond to the global, upper Asbian sea-level highstand and lower Brigantian sea-level lowstand, respectively (see Ramsbottom and Saunders 1985; Ross and Ross 1985). The lowstand segments of megacycles thus do not always fit the lowstand limbs on the global eustatic curve and, therefore, the eustatic forcing seems not to be the major control on the cyclic deposition. In addition, in the MF there is no support for development of condensed sections to overlie the basal lowstand turbidite systems (cf. Johnson et al. 2001). Instead, rather thick, low-efficiency fine-grained turbidite systems overlie the basal segments, indicating high rates of sediment supply.

Pulsating tectonic activity is considered to represent the most common control on deep-water foreland basin stratigraphy. It has been documented, for example, from the Tertiary Apennine foreland basin (Ricci-Lucchi 1986), Carboniferous foreland basin of the Pyrenees (Delvolvé et al. 1998) and the Carboniferous Rhenohercynian turbidite basin in Germany (Ricken et al. 2000). The pulsating tectonic control is usually associated with development of thrust highs that act as local source of clastic sediment supply to the deep basin (Ori et al. 1986). The thrust tectonics produce slope oversteepening and consequent mass wasting into the basin to form the typical asymmetric fining upward cycles (Mutti 1992). The orogenic belt in the hinterland of the MSCB was tectonically active during deposition of the MF, supporting plate convergence and tectonic forcing in the foreland. Maximum tectonic activity related to the exhumation of deep crustal Moldanubian complexes at 330 Ma (Schulmann et al. 1991) fits the time constraints of the Upper Viséan sedimentation of the MF (lower and upper absolute boundary of the Viséan are 334 and 325 Ma according to McKerrow and Van Staal 2000). The MSCB itself underwent large-scale overthrusting in the Lower Viséan to Westphalian period (Schulmann et al. 1991; Franců et al. 2002). The tectonic forcing mechanism can provide a reasonable explanation for the development of the basal sequence boundary and the overlying erosive channel systems typically comprising the basal megacycle segments. The deposition of distal fine-grained turbidites of the upper megacycle segments may then represent a return back to normal deposition of well-organized turbidite systems during a period of relative tectonic quiescence. However, Hartley and Otava (2001) refused tectonic forcing as the major control on the MSCB stratigraphy using high sediment supply rates and the presence of just one large point source as their main arguments. Given the absolute time limits for the Viséan (McKerrow and Van Staal 2000), the deposition of the MF (Goα1 to upper Goβ, about one-sixth to one-eighth of the whole Viséan) may have lasted for about 1.1 to 1.5 million years. This gives and average megacycle duration of about 0.5 to 0.8 million years and a rather high average sedimentation rate of about 1,200 to 1,600 m/Ma, which supports the previous high-sediment supply interpretations of Hartley and Otava (2001). However, the point source concept of Hartley and Otava (2001) is based largely on heavy-mineral provenance data. The MF was deposited during the Middle Heavy Mineral Zone dominated by pyrope-almandine rich garnets with a concomitant decrease in grossular content up-section, suggesting mostly metamorphic sources with an up-section trend towards even higher-grade metamorphic sources (Hartley and Otava 2001). Generally, our observations of sandstone and fine-grained conglomerate composition follow similar trends, but important local excursions were observed, such as the very high feldspar concentrations in sandstones at the base of megacycle 2, indicating a magmatic source (see discussion above), and the relatively high concentrations of sedimentary lithic grains at the base of segment 5 and at the base of megacycle 1 (Fig. 8). Supported by the presence of the proximal, channelized turbidite systems and slope aprons supplied from linear or multiple point source (segments 1, 3), the small-scale, sand-rich, point-sourced turbidite systems in the segment 4 and the lateral W–E palaeocurrent data, these data suggest a significant lateral input from the

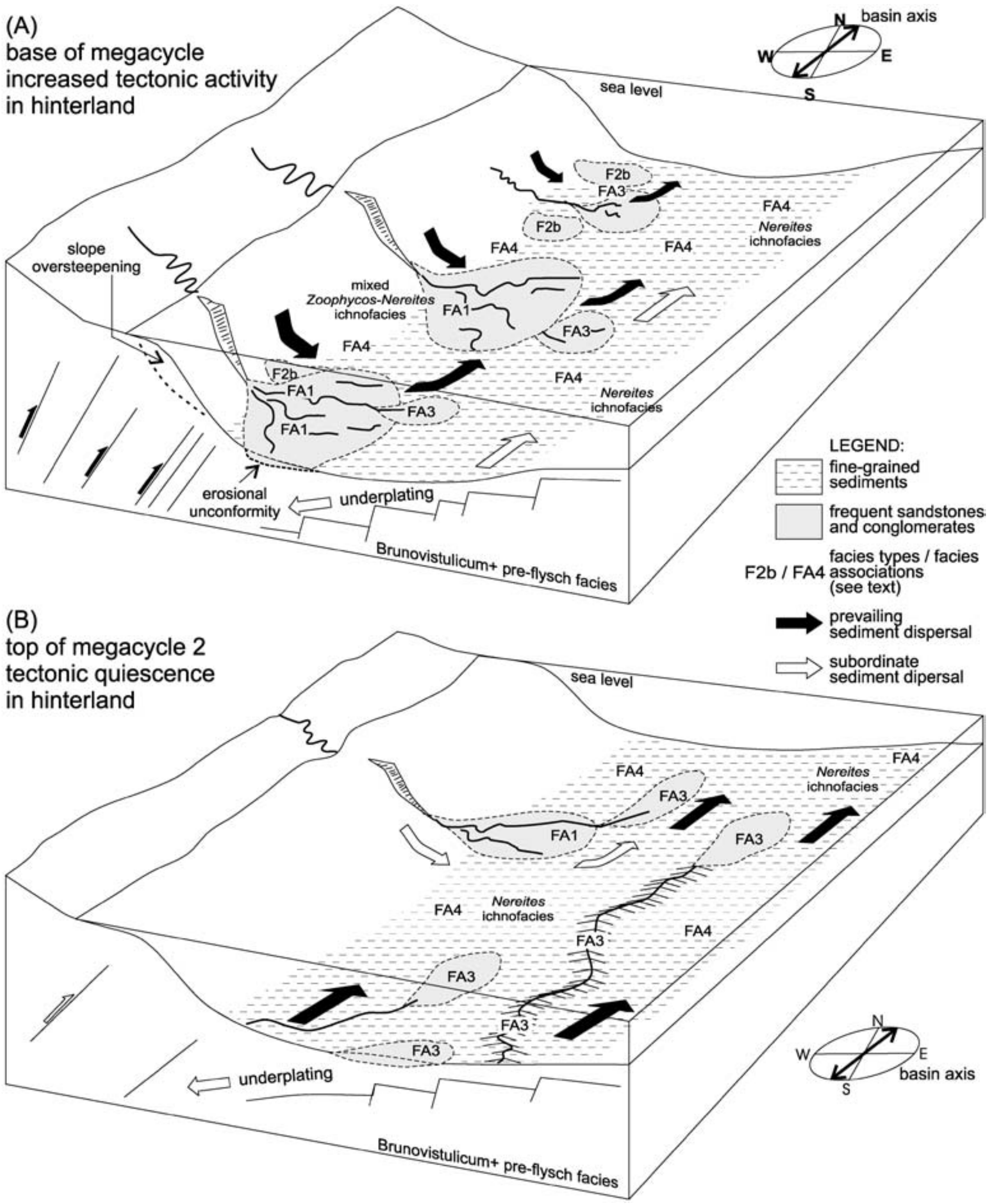

Fig. 9 A, B Tentative model of two-stage megacycle evolution of the MF based on changes in palaeoflow directions, distribution of facies associations and ichnofacies

orogenic wedge located in the (present-day) west (Fig. 9). The lateral input increased during deposition of the basal segments and decreased during deposition of the upper megacycle segments. Climatic control on cyclic turbidite sedimentation has been recently studied by Reeder et al. (2002) who suggested that cyclic patterns in turbidite systems may have resulted from climate changes in large river systems supplying sediment into the basin. The Lower Carboniferous is generally accepted to be a period of high climatic fluctuations related to Gondwana glaciation, but the rough time constraints of the MF deposits probably do not allow for climatic forcing to be evidenced from the facies analysis alone. The relatively high concentrations of potassium feldspars in the sandstones of the MF suggest short residence times in fluvial and nearshore environments. Consequently, very rapid sediment input is inferred, which probably overprinted the role of climatic fluctuations in controlling the hundred-metre scale cyclicity in the MF.

The interplay of high sediment supply from the southern point source and tectonic forcing in the western thrust-and-fold belt are possibly the major mechanisms controlling the cyclic stratigraphy of the Moravice Formation. Periods of increased tectonic activity in the hinterland produced slope oversteepening and uplift of local structural highs, resulting in development of a sequence boundary overlain by the basal, low-efficiency turbidite systems fed from the western multiple-source or linear source. During subsequent tectonic quiescence periods high-efficiency, fine-grained systems of the upper megacycle segments were established, which were fed predominantly from the southern point source, but the small-scale point-sourced, low-efficiency fans were possibly sourced from the west (Fig. 9).

Map distribution of lithotypes and outcrop data suggest that the segment 5 evolved from fine-grained high-efficiency system of the segment 4 by a gradual increase in proportion of the transitional channel-lobe and lobe sandstones (FA3). Segment 5 is not considered as another megacycle because its basal boundary is rather gradual than sharp and erosive, and the proximal turbidite systems are not present. The trend of rapid increase in quartz grain concentrations in the sandstones of segment 5 (Fig. 7 and 8) continues up-section to the even more quartzose sandstones and conglomerates of the overlying Hradec–Kyjovice Formation. The Hradec–Kyjovice Formation can be laterally correlated to sandstone and conglomerate facies in the southern Drahany Basin, which are thought to represent a major phase of fan progradation from the southern point source to the north (Hartley and Otava 2001, p. 147). Consequently, segment 5, marked by the increasing proportion of low-efficiency, sand-rich systems and increasing quartz concentrations in sandstones, may represent an initial phase of that progradation. Supported by the ichnofacies data suggesting better oxygenation of the depositional setting in segment 5, this shift may indicate a gradual transition from generally underfilled to generally overfilled systems in the MSCB.

Conclusions

The MF of the MSCB represents a multiphase, cyclic fill of a deep-water foreland basin with axial trough topography. In this respect, the MSCB shows a strong similarity with other Culm systems elsewhere in Europe, particularly with the (par)autochthonous Rhenohercynian Culm basin of Germany (Franke and Engel 1988; Ricken et al. 2000) and the Culm basin of the Pyrenees (Delvolvé et al. 1998). Compared with the MSCB, the English Culm basin (Hartley and Warr 1990; Burne 1995) seems to be rather oversupplied and does not show the characteristic, asymmetric cyclic stratigraphic arrangement.

Sediment composition data from the MF indicate an overall trend in decreasing supply from sedimentary/volcanic sources and increasing supply from plutonic/high-grade metamorphic sources up-section, which can be attributed to an uplift in the source area and progressive unroofing of its structurally deeper crustal parts. The general trend is consistent with the previous axial-dispersal model based on heavy mineral data (Hartley and Otava 2001), but our data indicate much higher lateral and vertical variability in sandstone and conglomerate composition, indicating variable lateral, W–E sediment input associated with periods of increased tectonic activity. Relatively high-diversity ichno-assemblages comprising some ‘shallow-marine’ ichnogenera occur for the first time in the uppermost part of the MF, being associated with sand-rich turbidite systems and accompanied by a rapid increase in quartz concentrations in sandstones. This interval is suggested to indicate a transition from a generally underfilled to a generally overfilled basin phase in the MSCB, being probably linked with the Upper Viséan major phase of northward basin-fill progradation assumed by previous authors.

For the most part, the MF comprises two asymmetric megacycles, each about 500 to 900 m thick and each comprising a time interval of about 0.5 to 0.8 million years, which implies high sedimentation rates of about 1,200 to 1,600 m/ma. The megacycles are bounded by a basal sequence boundary overlain by erosive low-efficiency, with relative coarse-grained turbidite systems indicating relative sea-level lowstand conditions. The basal lowstand systems pass up-section into about twice as thick distal, low-efficiency turbidite systems. A combined tectonic–sediment supply model is suggested that explains the cyclic stratigraphy. Periods of increased tectonic activity resulted in slope oversteepening, probably combined with increased rate of lateral, W–E sediment supply into the basin, producing the basal sequence boundary and the subsequent lowstand turbidite systems. During subsequent periods of tectonic quiescence the system was filled mainly from a distant southern point source, producing the thick, low-efficiency turbidite systems.

Acknowledgements This study was supported by GA CR Project No. 205/00/0118. Discussions with Jaromír Leichmann (Brno), Jiří Kalvoda (Brno), Alfred Uchman (Kraków) and David Uličný (Praha) during earlier phases of manuscript preparation are gratefully acknowledged. Thorough and very helpful reviews by journal reviewers Hilmar von Eynatten (Göttingen) and Jutta Winsemann (Hannover) and comments provided by Stuart Jones (Durham) helped to improve the manuscript significantly.

References

Agirrezabala LM, García-Mondéjar J (1994) A coarse grained turbidite system with morphotectonic control (middle Albian, Ondarroa, northern Iberia). Sedimentology 41:383–407

Bouma AH, Barnes NE, Normark WR (1985) Submarine fans and related turbidite systems. Springer, Berlin Heidelberg New York

Buatois LA, Angriman AOL (1992) The ichnology of a submarine braided channel complex: the Whisky Bay Formation, Cretaceous of James Ross island, Antarctica. Palaeogeogr Palaeoclim Palaeoecol 94:119–140

Burne RV (1995): The return of “The Fan That Never Was”: Westphalian turbidite system in the Variscan Culm Basin: Bude Formation (southwest England). In: Plint AG (ed) Sedimentary facies analysis. A tribute to the research and teaching of Harold G. Reading. Spec Publ Int Assoc Sediment 22:101–135

Carlson J, Grotzinger JP (2001) Submarine fan environment inferred from turbidite thickness distributions. Sedimentology 48:1331–1351

Cavazza W, DeCelles PG (1993) Geometry of a Miocene submarine canyon and associated sedimentary facies in southeastern Calabria, southern Italy. Geol Soc Am Bull 105:1297–1309

Ciner A, Deynoux M, Kosun E (1996) Cyclicity in the Middle Yamak turbidite complex of the Haymana basin, central Anatolia, Turkey. Geol Rundsch 85:669–682

Critelli S, Rumelhart PE, Ingersoll RV (1995) Petrofacies and provenance of the Puente Formation (Middle to Upper Miocene), Los Angeles basin, southern California: implications for rapid uplift and accumulation rates. J Sediment Res A65:656–667

Čížek P, Tomek Č (1991) Large-scale thin-skinned tectonics in the eastern boundary of the Bohemian Massif. Tectonics 10:273–286

Delvolvé JJ, Vachard D, Souquet P (1998): Stratigraphic record of thrust propagation, Carboniferous foreland basin, Pyrenees, with emphasis on Pays-de-Sault (France/Spain). Geol Rundsch 87:363–372

Dickinson WR (1985) Interpreting provenance relations from detrital modes of sandstones. In: Zuffa GG (ed) Provenance of Arenites. NATO Adv Ser C vol 148. Reidel, Dordrecht, pp 333–361

Dickinson WR, Beard LS, Brakenridge GR, Erjavec JL, Ferguson RC, Inman KF, Knepp RA, Lindberg FA, Ryberg PT (1983) Provenance of North American Phanerozoic sandstones in relation to tectonic setting. Geol Soc Am Bull 94:222–235

Dorsey RJ (1988) Provenance evolution and unroofing history of a modern arc-continent collision: evidence from petrography of Plio-Pleistocene sandstones, eastern Taiwan. J Sediment Petrol 58:208–218

Dvořák J (1995) Moravo–Silesian Zone; autochthon; stratigraphy. In: Dallmeyer RD, Franke W, Weber K (eds) Pre-Permian geology of central and eastern Europe. Springer, Berlin Heidelberg Berlin, pp 477–489

Dvořák J, Paproth E (1969) Ueber die Position und die Tektogenese des Rhenoherzynikums und des Sudetikums in den mitteleuropaeischen Varisziden. N Jahrbuch Geol Palaeontol Monatshefte 2:65–88

Ekdale AA, Manson TR (1988) Characteristic trace-fossil association in oxygen-poor sedimentary environments. Geology 16:720–723

Emery D, Myers KJ (1996) Sequence stratigraphy. Blackwell, Oxford

Falk PD, Dorsey RJ (1998) Rapid development of gravelly high-density turbidity currents in marine Gilbert-type fan deltas, Lorento Basin, Baja California Sur, Mexico. Sedimentology 45:331–349

Fergusson CL, Tye SC (1999) Provenance of early Palaeozoic sandstones, southeastern Australia. Part 1: vertical changes through the Bengal Fan-type deposit. Sediment Geol 125:135–151

Fillion D, Pickerill RK (1990) Ichnology of the Upper Cambrian? To Lower Ordovician Bell Island and Wabana groups of eastern Newfoundland, Canada. Palaeontogr Can 7:1–119

Franců E, Franců J, Kalvoda J, Poelchau HS, Otava J (2002) Burial and uplift history of the Palaeozoic Flysch in the Variscan foreland basin (SE Bohemian Massif, Czech Republic). EGS Stephen Mueller Spec Publ Ser 1:259–278

Franke W (1995) Rhenohercynian foldbelt; Autochthon and non-metamorphic nappe units; stratigraphy. In: Dallmeyer RD, Franke W, Weber K (eds) Pre-Permian geology of central and eastern Europe. Springer, Berlin Heidelberg New York, pp 33–49

Franke W, Engel W (1988) Tectonic settings of synorogenic sedimentation in the Variscan Belt of Europe. In: Besly BM, Kelling G (eds) Sedimentation in a synorogenic basin complex. The Upper Carboniferous of northwest Europe. Blackie, Glasgow, pp 8–17

Frey RW, Pemberton SG (1984) Trace fossils facies models. In: Walker RG (ed) Facies models, 2nd edn. Geoscience Canada, Ainsworth Press, Ontario, pp 189–207

Fritz H, Neubauer F (1995) Moravo–Silesian Zone; autochthon; structure. In: Dallmeyer RD, Franke W, Weber K (eds) Pre-Permian geology of central and eastern Europe. Springer, Berlin Heidelberg New York, pp 490–494

Fürsich FT (1974) On Diplocraterion Torrell 1870 and the significance of morphological features in vertical, spreite-bearing, U-shaped trace fossils. J Palaeontol 48:952–962

Hartley AJ, Otava J (2001) Sediment provenance and dispersal in a deep marine foreland basin: the Lower Carboniferous Culm Basin, Czech Republic. J Geol Soc Lond 158:137–150

Hartley AJ, Warr LN (1990) Upper Carboniferous foreland basin evolution in SW Britain. Proc Ussher Soc 7:211–216

Haughton PDW (2001) Evolving turbidite systems on a deforming basin floor, Tabernas, SE Spain. Sedimentology 47:497–518

Hickson TA, Lowe DR (2002) Facies architecture of a submarine fan channel-levee complex; the Juniper Ridge Conglomerate, Coalinga, California. Sedimentology 49:335–362

Hiscott RN, James NP (1985) Carbonate debris flows, Cow Head Group, western Newfoundland. J Sediment Petrol 55:735–745

Hiscott RN, Pickering KT, Beeden DR (1986) Progressive filling of a confined Middle Ordovician foreland basin associated with the Taconic Orogeny, Quebec, Canada. In: Allen PA, Homewood P (eds) Foreland basins. Int Assoc Sediment Spec Publ 8:309–325

Hofmann CC (1993) Trace fossils in Upper Carboniferous sediments of the Culm Basin and their implications for general depositional processes. Proc Ussher Soc 8:207

Houghton HF (1980) Refined techniques for staining plagioclase and alkali feldspars in thin section. J Sediment Petrol 50:629–631

Ingersoll RV, Fullard TF, Ford RL, Grimm JP, Pickle JD, Sares SW (1984) The effect of grain size on detrital modes; a test of the Gazzi–Dickinson point-counting method. J Sediment Petrol 54:103–116

Johnson SD, Flint S, Hinds D, Wickens HDV (2001) Anatomy, geometry and sequence stratigraphy of basin floor to slope turbidite systems, Tanqua Karoo, South Africa. Sedimentology 48:987–1023

Kneeler BC, Branney MJ (1995) Sustained high-density turbidity currents and the deposition of thick massive beds. Sedimentology 42:607–616

Kneller B, Buckee C (2000) The structure and fluid mechanics of turbidity currents; a review of some recent studies and their geological implications. Millennium reviews. Sedimentology 47:62–94

Kolla V (1993) Lowstand deep-water siliciclastic deposition systems: characteristics and terminologies in sequence stratigraphy and sedimentology. Bull Centres Rech Explor-Prod Elf Aquitaine 17:67–78

Kumpera O (1983) Lower Carboniferous geology of Jeseníky Block (in Czech). Knih Ústř Úst Geol 59

Kumpera O, Martinec P (1995) The development of the Carboniferous accretionary wedge in the Moravian–Silesian Paleozoic Basin. J Czech Geol Soc 40:47–60

Leverenz A (2000) Trench sedimentation versus accreted submarine fan: an approach to regional-scale facies analysis in a Mesozoic accretionary complex: "Torlesse" terrane, northeastern North Island, New Zealand. Sediment Geol 132:125–160

Lewis KB, Barnes PM (1999) Kaikoura Canyon, New Zealand; active conduit from near-shore sediment zones to trench-axis channel. Mar Geol 162:39–69

Lombard A (1963) Laminites: a structure of flysch type sediments. J Sediment Petrol 33:14–22

Lowe DR (1982) Sediment gravity flows: II. Depositional models with special reference to the deposits of high-density turbidity currents. J Sediment Petrol 52:279–297

Mattern F (2002) Amalgamation surfaces, bed thicknesses, and dish structures in sand-rich submarine fans; numeric differences in channelized and unchanellized deposits and their diagnostic value. Sediment Geol 150:203–228

McKerrow WS, Van Staal CR (2000) The Palaeozoic time scale reviewed. In: Franke W, Haak V, Oncken O, Tanner D (eds) Orogenic processes: quantification and modelling in the Variscan Belt. Geol Soc Spec Publ 179:5–8

Middleton GV, Hampton MA (1973) Sediment gravity flows: mechanics of flow and deposition. In: Middleton GV, Bouma AH (eds) Turbidites and deep water sedimentation. Soc Econ Paleontol Mineral Short Course Notes

Mikuláš R, Lehotský T, Bábek O (2002) Ichnofabric of the Culm facies: a case study of the Moravice Formation (Lower Carboniferous; Moravia and Silesia, Czech Republic). Geol Carpathica 53:141–148

Mulder T, Alexander J (2001) The physical character of subaqueous sedimentary density flows and their deposits. Sedimentology 48:269–299

Mulder T, Migeon S, Savoye B, Faugères J-C (2001) Inversely graded turbidite sequences in the deep Mediterranean: a record of deposits from flood-generated turbidity currents? Geo-Mar Lett 21:86–93

Mutti E (1992) Turbidite sandstones. Agip SpA S Donato Milanese

Mutti E, Normark WR (1987) Comparing examples of modern and ancient turbidite systems: problems and concepts. In: Leggett JK, Zuffa GG (eds) Marine clastic sedimentology; concepts and case studies. Graham and Trotman, London, pp 1–38

Mutti E, Ricci-Lucchi F (1975) Turbidite facies and facies associations. In: Mutti E et al. (eds) Examples of turbidite facies and facies associations from selected formations in the Northern Apennines, field trip guidebook A-11. Int Congress Sedimentologists Nice, pp 21–36

Mutti E, Sonnino M (1981) Compensation cycles: a diagnostic feature of turbidite sandstone lobes. In Abstract Volume, 2nd International Association Sedimentologists European Regional Meeting, Bologna, pp 120–123

Normark WR, Piper DJW (1991) Initiation processes and flow evolution of turbidity currents; implications for the depositional record. In: Osborne RH (ed) From shoreline to abyss; contributions in marine geology in honor of Francis Parker Shepard. Soc Econ Paleontol Mineral Spec Publ 46:207–230

Normark WR, Piper DJW, Hiscott RN (1998) Sea level control on textural characteristics and depositional architecture of the Hueneme and associated submarine fan systems, Santa Monica Basin, California. Sedimentology 45:53–70

Ori GG, Roveri M, Vannoni F (1986) Plio-Pleistocene sedimentation in the Apenninic–Adriatic foredeep (central Adriatic sea, Italy). In: Allen PA, Homewood P (eds) Foreland basins. Int Assoc Sedimentologists Spec Publ 8. Blackwell, Oxford, pp 183–198

Orr PJ (2001) Colonization of the deep-marine environment during the early Phanerozoic: the ichnofaunal record. Geol J 36:265–278

Pemberton GS, Frey RW (1982) Trace fossils nomenclature and the Planolites–Palaeophycus dilemma. J Paleontol 56:843–881

Pfeiffer H (1969) Die spurenfossilien des Kulms (Dinants) und devons der Frankenwäjder Querzone (Thüringen). Jb Geol 2:651–717

Pickering KT, Hiscott RN (1985) Contained (reflected) turbidity currents from the Middle Ordovician Cloridorme Formation, Quebec, Canada; an alternative to the antidune hypothesis. Sedimentology 32:373–394

Pickering KT, Hodgson DM, Platzman E, Clark JD, Stephens C (2001) A new type of bedform produced by backfilling processes in a submarine channel, late Miocene, Tabernas-Sorbas Basin, SE Spain. J Sediment Res 71:692–704

Piper DJW, Stow DAV (1991) Fine-grained turbidites. In: Einsele G, Ricken W, Seilacher A (eds) Cycles and events in stratigraphy. Springer, Berlin Heidelberg New York, pp 360–376

Plička M (1970) Zoophycos and similar fossils. In: Crimes TP, Harper JC (eds) Trace fossils. J Geol Spec Pap 3:361–370

Plink-Björklund P, Mellere D, Steel RJ (2001) Turbidite variability and architecture of sand-prone, deep-water slopes; Eocene clinoforms in the Central Basin, Spitsbergen. J Sediment Res 71:895–912

Posamentier HW, Vail PR (1988) Eustatic controls on clastic deposition II: sequence and systems-tract models. Soc Econ Paleontol Mineral Spec Publ 42:125–154

Posamentier HW, Erskine RD, Mitchum RM (1991) Models for submarine fan deposition within a sequence stratigraphic framework. In: Weimer P, Link MH (eds) Seismic facies and sedimentary processes of modern and ancient submarine fans and turbidite systems. Springer, Berlin Heidelberg New York, pp 127–136

Rajlich P (1989) Strain and tectonic styles related to Variscan transpression and transtension in the Moravo–Silesian Culmian basin, Bohemian Massif, Czechoslovakia. Tectonophysics 174:351–367

Ramsbottom WHC, Saunders WB (1985) Evolution and evolutionary biostratigraphy of Carboniferous ammonoids. J Paleontol 59:123–139

Reading HG, Richards MT (1994) Turbidite systems in deep water basin margins classified by grain-size and feeder system. Am Assoc Petrol Geol Bull 78:792–822

Reeder MS, Stow DAV, Rothwell RG (2002) Late Quaternary turbidite input into the east Mediterranean basin: new radiocarbon constraints on climate and sea-level control. In: Jones SJ, Frostick LE (eds) Sediment flux to basins: causes, controls and consequences. Geol Soc Spec Publ 191:267–278

Rhoads DC, Boyer LF (1982) The effects of marine benthos on physical properties of sediments: a successional perspective. In: McCall PL, Tevesz MJS (eds) Animal–sediment relations. The biogenic alteration of sediments. Topics Geobiol pp 3–52

Ricci-Lucchi F (1986) The Oligocene to Recent foreland basins of the northern Apennines. In: Allen PA, Homewood P (eds) Foreland basins. Int Ass Sediment Spec Publ 8:105–139

Ricken W, Schrader S, Oncken O, Pletsch A (2000) Turbidite basin and mass dynamics related to orogenic wedge growth; the Rheno-Hercynian case. In: Franke W, Haak V, Oncken O, Tanner D (eds) Orogenic processes: quantification and modelling in the Variscan Belt. Geol Soc Spec Publ 179:257–280

Ross CA, Ross RP (1985) Late Paleozoic depositional sequences are synchronous and worldwide. Geology 13:194–197

Rothwell RG, Pearce TJ, Weaver PPE (1992) Late Quaternary evolution of the Madeira abyssal plain, Canary Basin, NE Atlantic. Basin Research 4:103–131

Schulmann K, Ledru P, Autran A, Melka R, Lardeaux JM, Urban M, Lobkowicz M (1991) Evolution of nappes in the eastern margin of the Bohemian Massif; a kinematic interpretation. Geol Rundsch 80:73–92

Seilacher A (1967) Bathymetry of trace fossils. Mar Geol 5:413–428

Shanmugam G (1980) Rhythms in deep sea, fine-grained turbidite and debris flow sequences, Middle Ordovician, eastern Tennessee. Sedimentology 27:419–432

Shanmugam G (1996) High-density turbidity currents: are they sandy debris flows? J Sediment Res 66:2-10

Shanmugam G, Moiola RJ (1985) Submarine fan models: problems and solutions. In: Bouma AH, Normark WR, Barnes NE (eds) Submarine fans and related turbidite systems. Springer, Berlin Heidelberg New York, pp 29–34

Shanmugam G, Moiola RJ (1995) Reinterpretation of depositional processes in a classic flysch sequence (Pennsylvanian Jackfork Group), Quachita Mountains, Arkansas and Oklahoma. Am Assoc Petrol Geol Bull 79:672–695

Sinclair HD (2000) Delta-fed turbidites infilling topographically complex basins: a new depositional model for the Annot Sandstones, SE France. J Sediment Res 70:504–519

Sohn YK (2001) Depositional processes of submarine debris flows in the Miocene fan deltas, Pohang Basin, SE Korea with special reference to flow transformation. J Sediment Res 70:491–503

Sohn YK, Rhee CW, Shon H (2001) Revised stratigraphy and reinterpretation of the Miocene Pohang basinfill, SE Korea; sequence development in response to tectonism and eustasy in a back-arc basin margin. Sediment Geol 143:265–285

Stepanek J, Geyer G (1989) Spurenfossilien aus dem Kulm (Unterkarbon) des Frankenwaldes. Beringeria 1:1–55

Stow DAV (1979) Distinguishing between fine-grained turbidites and contourites on the Nova Scotian deep water margin. Sedimentology 26:371–384

Surlyk F (1987) Slope and deep shelf gully sandstones, Upper Jurassic, East Greenland. Am Assoc Petrol Geol Bull 71:464–475

von Eynatten H, Gaupp R (1999) Provenance of Cretaceous synorogenic sandstones in the Eastern Alps: constraints from framework petrography, heavy mineral analysis and mineral chemistry. Sediment Geol 124:81–111

Walker RG (1965) The origin and significance of the internal sedimentary structures of turbidites. Proc Yorkshire Geol Soc 35:1–32

Weimer P, Varnai P, Budhijanto FM, Acosta ZM, Martinez RE, Navarro,AF, Rowan,MG, McBride BC, Villamil T, Arango C, Crews JR, Pulham AJ (1998) Sequence stratigraphy of Pliocene and Pleistocene turbidite systems, northern Green Canyon and Ewing Bank (offshore Louisiana), northern Gulf of Mexico. Am Assoc Petrol Geol Bull 82:918–960

Wetzel A, Werner F (1981) Morphology and ecological significance of Zoophycos in deep-sea sediments of NW Africa. Palaeogeogr Palaeoecol Palaeoclimatol 32:182–212

Zapletal J (1986) Paraconglomerates of Moravice Formation from Bílčice (Nízký Jeseník Mts) (In Czech). Čas Slez Muz Opava (A) 35:171–182

Zapletal J, Pek I (1999) Ichnofacies of the Lower Carboniferous in the Jesenik Culm (Moravo-Silesian region, Bohemian Massif, Czech Republic). Bull Czech Geol Surv 74:343–346

Zuffa GG (1985) Optical analyses of arenites: influence of methodology on compositional results. In: Zuffa GG (ed) Provenance of Arenites. NATO Adv Ser C vol 148. Reidel, Dordrecht, pp 165–189